ADVISORY GROUP FOR AERONAUTICAL RESEARCH AND DEVELOPMENT

64 RUE DE VARENNE, PARIS VII

REPORT 453

WALL-PRESSURE FLUCTUATIONS AND PRESSURE-VELOCITY CORRELATIONS IN TURBULENT BOUNDARY LAYERS

by

JOHN S. SERAFINI

APRIL 1963

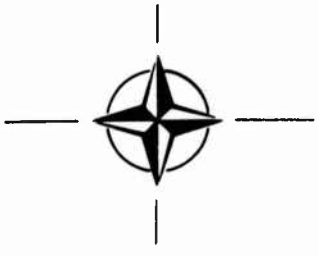

NORTH ATLANTIC TREATY ORGANIZATION

REPORT 453

NORTH ATLANTIC TREATY ORGANIZATION

ADVISORY GROUP FOR AERONAUTICAL RESEARCH AND DEVELOPMENT

WALL-PRESSURE FLUCTUATIONS AND PRESSURE-VELOCITY CORRELATIONS IN TURBULENT BOUNDARY LAYERS

by

John S. Serafini

This Report is one in the Series 448-469 inclusive, presenting papers, with discussions, given at the AGARD Specialists' Meeting on 'The Mechanism of Noise Generation in Turbulent Flow' at the Training Center for Experimental Aerodynamics, Rhode-Saint-Genèse, Belgium, 1-5 April 1963, sponsored by the AGARD Fluid Dynamics Panel

SUMMARY

Pressure fluctuations of a turbulent layer along a plane boundary have been investigated experimentally. All measurements were made at a nominal free-stream Mach number of 0.6 and an average Reynolds number per foot of 3.45×10^6 in a wind-tunnel facility specially designed for the purpose. The pressure fluctuations were measured with miniature pressure transducers and the velocity fluctuations with hot-wire anemometers.

The root-mean-square magnitudes of the wall-pressure fluctuations agree with the Lilley-Hodgson theoretical results, whereas the mean-square spectra do not agree, except over a small range of frequencies. Space-time correlations of the wall-pressure fluctuations generally agree with Willmarth's experimental results for longitudinal separation distances. Measurements of lateral space-time correlations indicated that the ratio of the longitudinal to lateral length-scale is approximately 7.4. The convection velocity of the fluctuations is found to increase with increasing separation distances and its significance is explained.

Measurements of the correlations of the wall-pressure fluctuations with the longitudinal component of the velocity fluctuations indicate that the contributions to the wall-pressure fluctuations are from two regions, an inner region near the wall and an outer region linked with the intermittency.

532.526.4

3b2f: 3b2e1a

SOMMAIRE

On a procédé à une recherche expérimentale sur les fluctuations de pression d'une couche turbulente le long de la limite d'un avion. Toutes les mesures ont été établies pour un nombre de Mach courant libre de 0,6 et à indice Reynolds moyen par pied (30,5 cm) de $3,45 \times 10^6$, dans un tunnel aérodynamique spécialement réalisé dans ce but. Les fluctuations de pression ont été mesurées à l'aide de transducteurs à pression miniature, et les fluctuations de vitesse avec des anémomètres à fil chaud.

Les grandeurs de racine de la moyenne des carrés des fluctuations de pression aux parois concordent avec les résultats théoriques de Lilley-Hodgson, alors que les spectres de moyenne des carrés ne concordent pas, sauf sur une faible plage de fréquences. Les corrélations espace-temps des fluctuations de pression aux parois s'accordent en général avec les résultats expérimentaux de Willmarth pour des distances de séparation longitudinales. Les mesures de corrélations espace-temps latérales dénotaient que le rapport des échelles de longueurs longitudinale et latérale est d'à peu près 7,4. La vitesse de convection des fluctuations, d'après ce que l'on constate, croît avec l'augmentation des distances de séparation et l'on explique son importance.

Les mesures de corrélations des fluctuations de pression aux parois et de la composante longitudinale des fluctuations de vitesse indiquent que les contributions aux fluctuations de pression aux parois proviennent de deux régions, une région intérieure proche de la paroi et une région extérieure liée à l'intermittence.

532.526.4

3b2f:3b2e1a

CONTENTS

LIST OF TABLES

LIST OF FIGURES

NOTATION

a	speed of sound (ft/sec)
c_f	local skin-friction coefficient defined as local viscous shear stress at wall divided by dynamic pressure evaluated at free-stream conditions (dimensionless)
d	diameter of pressure transducers (in.)
$F(f)$	spectrum function, $\sqrt{\left(\overline{p^2(f)}\right)}\Big/\sqrt{\left(\overline{p^2}\right)}$ $[(\text{sec})^{1/2}]$
$\Im(f)$	spectral-density function, $\overline{p^2(f)}\Big/\overline{p^2}$ or $\int_0^\infty \Im(f)df = 1$ (sec)
$\Im(k)$	$\frac{U}{2\pi}\Im(f)$ (cm)
f	frequency (sec^{-1})
H	ratio of δ^* to the momentum thickness θ of boundary layer, dimensionless
k	wave number, $2\pi f/U$ (cm^{-1})
L_{p_x}	typical length scale of wall-pressure fluctuations in x-direction (in.)
L_{p_y}	typical length scale of wall-pressure fluctuations in y-direction (in.)
M	Mach number, U/a (dimensionless)
p	fluctuating static-pressure $(\text{lb/ft}^2$ or $\text{dynes/cm}^2)$
$\overline{p^2(f)}$	mean-square pressure fluctuation per unit bandwidth $\left(\text{as defined by } \overline{p^2} = \int_0^\infty \overline{p^2(f)}df\right)$ $[(\text{lb}^2)(\text{sec})/\text{ft}^4]$
$\tilde{p}(\omega)$	abbreviated notation following Willmarth[19]; also written as $\overline{p^2(\omega)} = \frac{1}{2\pi}\overline{p^2(f)}$
q	dynamic pressure, $\frac{1}{2}\rho U^2$ (lb/ft^2)
R	wall-pressure correlation coefficient (see equ. 2) (dimensionless)
$\mathcal{R}$	pressure-velocity correlation coefficient, $\overline{pu}\Big/\sqrt{\left(\overline{p^2}\right)}\sqrt{\left(\overline{u^2}\right)}$ (dimensionless)
Re_x	Reynolds number based on equivalent distance of boundary-layer development $(x - x_0)$ with $x_0 = -2.1$ ft (obtained from δ^* as a function of x) (dimensionless)

Re_θ	Reynolds number based on momentum thickness (dimensionless)
SPL	$= 20 \log_{10} \left(\sqrt{\overline{p^2}} / p_0 \right)$, where p_0 is a reference pressure equal to 2×10^{-4} (dynes/cm^2, db)
t	time (sec)
$U = U_1$	longitudinal component of mean velocity (i.e. $\overline{U + u} = \bar{U} \equiv U$), (ft/sec)
$u = u_1$	longitudinal component of turbulent or fluctuating velocity, (ft/sec)
$V = U_2$	transverse component of mean velocity (V assumed to be negligible in boundary layer) [ft/sec]
$v = v_2$	transverse component of fluctuating velocity, ft/sec
$W = U_3$	normal (to wall) component of mean velocity (W assumed to be negligible in boundary layer) [ft/sec]
$w = u_3$	normal (to wall) component of fluctuating velocity (ft/sec)
x	vector in x-y-z coordinate space (ft)
$x = x_1$	longitudinal coordinate (parallel to wind-tunnel centerline and taken as positive in direction of flow and with $x_1 = 0$ at beginning of test section) [ft]
$y = x_2$	transverse coordinate (ft or in.)
$z = x_3$	normal (to wall) coordinate (ft or in.)
β	proportionality constant between r.m.s. wall-pressure fluctuations and local skin-friction coefficient (Equ. 1) [dimensionless]
γ	intermittency factor defined as average time that signal is turbulent divided by total time (dimensionless)
δ	boundary-layer thickness (in.)
δ^*	displacement thickness, as defined in Ref. 31 (p. 291) [in.]
ζ	separation distances in z-direction (in.)
η	separation distances in y-direction (in.)
θ	momentum thickness as defined in Ref. 31 (p. 291) [in.]
ξ	relative distances in x-direction (in.)
ρ	density of air (slugs/ft^3)

τ	time delay, i.e. difference between two instants of time (sec or msec)
ω	frequency, $2\pi f$, (radians/sec)

Subscripts

c	convection
opt	refers to value of correlation coefficient and time delay associated with peak in correlation curve that occurs nearest $\tau = 0$
p	pressure
s	refers to value of correlation coefficient and time delay for peak in correlation curve that occurs near $\tau = -1$ msec
w	wall
∞	free-stream condition

Superscript

$(\bar{})$	time averaged, $\bar{\alpha} = \lim_{T\to\infty}\left[\frac{1}{T}\int_0^T \alpha(t)dt\right]$

WALL-PRESSURE FLUCTUATIONS AND PRESSURE-VELOCITY CORRELATIONS IN TURBULENT BOUNDARY LAYERS

John S. Serafini*

1. INTRODUCTION

In recent years some interest has been shown in determining the characteristics of pressure fluctuations associated with turbulence. The interest in the characteristics of fluctuating pressures has come about as a result of the problems created by high levels of aerodynamic noise from powerful jet engines and high-speed aircraft. Even though the resulting research has been aimed at describing phenomenologically the turbulent flows in order to calculate the radiated noise, the study of the pressure fluctuations and their relation to the turbulent velocities is fundamental. Such is the case for turbulent flow fields exhibiting a mean shear and exposed to a bounding surface, for example, the turbulent plane wall boundary layer.

The first definitive works on the general problem of aerodynamic noise generated by a fluctuating velocity field without confining boundaries are the two classical theoretical papers by Lighthill[1, 2]. The work by Lighthill stimulated a series of papers (based on his theory) that studied the aerodynamic noise generated by particular turbulent flows[3, 11]. All these papers are concerned with the aerodynamic noise radiated from a turbulent region of flow.

The pressure fluctuations intrinsic to a turbulent field can, in principle, be determined if the basic equations of motion and continuity are satisfied for a fluid assumed to be incompressible and Stokesian. The pressure fluctuations from homogeneous, isotropic turbulence have been considered by Heisenberg[12] and Batchelor[13]. The fluctuating pressure field within homogeneous anisotropic turbulence was determined by Kraichnan[14]. The first attempt to determine the wall-pressure fluctuations for a turbulent-boundary-layer flow over a plane boundary was by Kraichnan[15]. In particular, Kraichnan showed that $\sqrt{\left(\overline{p_w^2}\right)}\Big/q_\infty \approx \beta c_f$, where β is a factor between 2 and 12. Lilley and Hodgson[16] used an analysis similar in method to that of Kraichnan[15], but depending on a slightly different model. In a subsequent paper Lilley[17] presented a more exact analysis resulting in $\sqrt{\left(\overline{p_w^2}\right)}\Big/q_\infty \approx 3.1\ c_f$.

The experimental work on the characteristics of pressure fluctuations in turbulent flows has been limited to measurements of fluctuating pressures on surfaces bounding the turbulence. In Reference 18, from measurements of the fluctuating wall-pressures of the turbulent boundary layer in a wind-tunnel at velocities between 50 and 200 ft/sec, a value of 0.8 was determined for the effective convective velocity of the pressure fluctuations divided by the free-stream velocity. Willmarth[19] has made measurements with an improved pressure transducer of the wall-pressure fluctuations presented in dimensionless form. His space-time correlations confirmed the existence of the convective pattern of the pressure fluctuations. Skudrzyk and Haddle[20] present wall-pressure fluctuation measurements along with aerodynamic noise

* *National Aeronautics and Space Administration, Lewis Research Center, Cleveland, Ohio, U.S.A.*

measurements in a water tunnel for smooth and rough surfaces. In Reference 21 some measurements are presented of the longitudinal space-time correlations of wall-pressure fluctuations in turbulent pipe flow.

The previously mentioned theoretical papers[14-17] and experimental papers[18-21] have indeed resulted in considerable contributions toward determining the behavior of the wall-pressure fluctuations. It was felt that a need existed for additional experimental data taken for a plane wall turbulent boundary layer under carefully controlled flow conditions, and that measurements should be taken which attempt to relate the wall-pressure fluctuations to at least some of the characteristics of turbulence within the turbulent layer itself.

The present work is primarily an experimental study of the wall-pressure fluctuations of a turbulent boundary layer and of their relation to the turbulent velocities within the layer.

The magnitude and frequency spectral distributions of the wall-pressure fluctuations have been measured with three pressure transducers. These transducers have different effective sensitive areas and include two different types - piezoelectric ceramic and capacitive diaphragm. The results are compared with other reported measurements. Space-time correlations of the wall-pressure fluctuations have been made with the use of piezoelectric ceramic transducers. Data were obtained with the line connecting the transducers making an angle of 0°, 45°, and 90° with respect to the free-stream velocity. These measurements are analyzed with the intent of relating them to the velocity characteristics of the layer. In an attempt to relate more precisely the wall-pressure fluctuations to the velocity fluctuations of the layer, correlations of the wall-pressure transducer signals and hot-wire signals are presented and discussed. Additional details of the work presented herein are contained in Reference 22.

2. APPARATUS AND PROCEDURE

All the measurements were made of the turbulent boundary layers on one inside wall of the test section of a continuous-suction nonreturn wind tunnel specially designed for this investigation (Fig.1). The airflow was drawn from a very large room (with access to outside air) through a set of filters at the inlet and through a contraction section into the test section. The test section had porous inner walls on three sides to remove some of the low-energy boundary-layer air all along the side opposite the measured boundary layer and to remove it partially on the two sides adjacent to the measured boundary layer. The net result was that the longitudinal static-pressure gradient could be adjusted to be zero or even adverse.

At the exit of the test section was a vibration-isolation section after which the airflow was choked by an area-constricting section, which is designated as a control block. It controls the mean flow in the test section and prevents any undesirable noises that may occur in the piping to the exhausting machinery from being propagated acoustically upstream into the test section. For further details on the wind-tunnel facility refer to Reference 22, which describes it more fully.

The mean Mach number in the wind tunnel was set at 0.6. The suction flow through the porous walls was controlled to give a slightly favorable longitudinal static-pressure

gradient for most of the experiments. The stagnation conditions at the inlet were atmospheric pressure and temperature. For the entire set of experiments the stagnation pressure and temperature ranged from 28.98 to 29.54 inches of mercury, and from 35° to 87° F, respectively. During any given experiment the maximum variation in stagnation pressure and temperature was ±0.04 inch of mercury and ±7° F, respectively. The exhaust pressure was maintained at approximately 10 inches of mercury absolute.

The mean velocity profiles of the turbulent boundary layer adjacent to the solid wall were computed from measurements made at stations along the test section with an automatically activated total-pressure probe. These measurements were used to calculate the boundary-layer parameters such as δ^*, θ, H, Re_θ, and c_f, which was calculated from the Ludwig-Tillman equation[23].

The pressure fluctuations were measured with two types of pressure transducers. These were the commercially available capacity-type transducers (Altec-Lansing Condenser Microphones) and a series of piezoelectric ceramic transducers which were developed specifically for the envisioned tasks. Table I briefly lists certain characteristics of the pressure transducers used along with alphabetic designations. A detailed description of both types of these transducers, their use, and calibration is given in Reference 22.

In Figure 2 a sketch is presented of a piezoelectric pressure transducer. The shape of the piezoelectric elements used is an annular circular cylinder of the radially polarized length expander type. The cap cemented on the end of the element greatly increases the area on which the forces act. In the case of wall-pressure fluctuation transducers, an end cap is vital in order not to disturb the boundary layer flow. No means of vibration isolation was provided, since it was not needed. The amplifier used with the piezoelectric transducers was a Decade Isolation Amplifier, Model 102B (manufactured by Keithley Instruments, Inc.), because of its high input impedance, low output impedance, and very accurate gains over a wide bandwidth. The cables and connectors used were of a low-noise miniature type.

The mean-square wall-pressure fluctuations were measured at various points along the wall with two transducers - piezoelectric transducer ZR and condenser transducer CA. For the space-time correlations of wall-pressure fluctuations, matched pairs of 0.125-inch-diameter piezoelectric pressure transducers were used. The minimum transducer separation distance was 0.181 inch and the maximum was 6.235 inches. The 8-inch-diameter port in which the pairs were mounted could be rotated in the plane of the wall. Measurements were made at angles of 0°, 45°, and 90° to the stream velocity. In the case of the correlations of velocity and wall-pressure fluctuations both transducers ZS and CB were used. The spatial relation of the hot-wire and the pressure transducer is indicated in Figure 3.

The velocity fluctuations were measured with the use of a constant-temperature hot-wire anemometer system described in References 24, 25 and 26. The hot-wire element used to sense the flow fluctuations was a tungsten wire with a diameter of 2×10^{-4} inch and an unplated or sensitive length of 0.080 inch. A description of the method of obtaining and evaluating the hot-wire data obtained herein is given in Reference 22 along with some comments on the use of the hot-wire anemometer. The stream component of the fluctuating velocity in the boundary layer was measured at several stations along the test section to establish the development of the turbulent boundary layer.

The most important use of the hot-wire probes was in obtaining the correlations of the wall-pressure and velocity fluctuations. In this case several hot-wire probes of slightly different distances from prong tips to probe centerline (see Fig.3) were used. This made it possible to make measurements of the correlation between the wall-pressure and velocity fluctuations where the hot-wire and the pressure transducer were separated by several streamwise distances ξ as measured in the plane of the wall and noted in Figure 3. Separation distances η, where η is measured normal to the stream velocity vector and in the plane of the wall (Fig.3(b)), were obtained by first rotating the hot-wire probe to get the desired separation η and then rotating the 8-inch-diameter port, within which both the pressure transducer and hot-wire probe were installed, until the axis of the hot-wire probe was again parallel to the stream velocity vector, that is, the test-section longitudinal centerline. The relative position of the hot-wire and pressure transducer in the plane of the wall was set, viewed, and photographed by means of a specially built camera setup that allowed optical magnifications by a factor of 10 or more.

For all the various types of measurements, after first establishing steady-state flow conditions in the wind tunnel, the total temperature and pressure and static pressures were recorded and subsequently monitored during the entire survey. The instrumentation for obtaining and analyzing the data on the velocity and pressure fluctuations is indicated by the schematic diagrams in Figure 4. The electrical voltages resulting from these fluctuations were measured on true r.m.s. voltmeters, recorded on a one-tenth-decade spectrum analyzer and level recorder and also recorded on a dual-channel tape recorder. In the case of the hot-wire probes, the d-c component of bridge voltage and the amount of bridge unbalance were also noted.

The spectrum analyzer and level recorder automatically scanned a set of filters centered on frequencies of 16 to 32,000 cycles/sec. Each filter set gave a one-tenth-decade band pass. The spectrum analyzer was used not only to measure the spectrum of the fluctuating velocities and wall pressures for the purpose of presenting them herein, but also to monitor the functioning of all the transducers during the tape recording of the fluctuating signals to be used for correlations.

The correlation measurements were obtained by processing the recorded signals through a playback unit which allowed one magnetic head to be moved with respect to the other to introduce a time delay between the two signals. These two signals were electronically multiplied. The electrical voltage outputs representing the correlation coefficient and the time-delay were then plotted on an X-Y recorder. Reference 22 describes in greater detail the instrumentation and procedure for obtaining the correlations of the wall-pressure fluctuations and those of the wall-pressure fluctuations with the velocity fluctuations.

3. RESULTS

The mean free-stream Mach number M_∞ in the wind tunnel for the entire set of experiments was 0.6. The static pressure exhibited slight variations, since for a given Mach number its value naturally depended on the total or atmospheric pressure. A typical variation of M_∞ and static pressure with longitudinal distance in the test section is presented in Figure 5. It should be noted that, although the static-pressure gradient is slightly favorable throughout the test section, there is

a small decrease of total pressure at large downstream positions. The Mach number does not continue to increase slightly with x but levels out and then slightly decreases with x. The mean Reynolds number per foot was 3.45×10^6 referred to the free-stream velocity. Since no significant differences were noticed in the pressure fluctuations for the static-pressure gradient being zero or slightly favorable, all the reported results are only for the latter case.

3.1 Velocity Characteristics of Measured Boundary Layer

Typical velocity profiles throughout the boundary layer obtained with a pitot tube are given in Figure 6. Figure 6(a) shows profiles for z plotted against M for two stations at which measurements were later made of the magnitude and spectra of the wall-pressure fluctuations, but which were upstream of the station used for correlation measurements. In Figure 6(b) these two velocity profiles, along with two other velocity profiles further downstream, are given in terms of the dimensionless quantities z/δ against U/U_∞. The dimensionless profiles are plotted in Figure 6(b) to compare roughly the state of development at the various stations, and it is seen that no appreciable change in the dimensionless profile occurs downstream of the second station, $x = 9.75$ feet.

The variation of δ^* as a function of the station x is given in Figure 7. Since the data exhibit some scatter, in subsequent calculations to nondimensionalize the magnitudes and frequencies of the pressure-fluctuation measurements, the values from the faired curve were used. Local skin-friction coefficients calculated from measured values of δ^*, θ, H, and Re_θ by means of the Ludwig-Tillman equation[23] are given in Figure 8 as a function of Re_x. Also shown in this Figure is the curve of the Prandtl-Schlichting equation (see Ref.27, p.438, footnote).

Figure 9 presents a typical boundary-layer profile of the longitudinal turbulent intensity. Figure 10 shows the maximum turbulent intensity of the profiles such as that given in Figure 9 as a function of the Reynolds number based on the distance along the wall, or Re_x. It is interesting to note that, although small in magnitude, there is an increase in the maximum turbulent intensity with Re_x. Also shown in Figure 10 is the value of turbulent intensity for the largest values of z possible with the available probe actuator (approx. 3.8 in. from the solid wall, thus close to the centerline of the tunnel). This centerline value exhibits a very slight increase similar to the maximum turbulent intensity data and a second increase in the downstream portion of the test section.

The measurements of the mean-flow profiles (Fig.6) and u-fluctuation profiles (Figs.9 and 10) indicate that a typical turbulent boundary layer is obtained. Although Figure 6 shows that its development is not entirely complete for the station $x = 2.75$ feet and is complete by $x = 9.75$ feet, Figure 10 indicates a high level of maximum turbulent intensity, even at these upstream stations. At $x = 2.75$ feet ($Re_x = 10 \times 10^6$) the turbulent intensity $\sqrt{(\overline{u^2})}/U_\infty$ is 0.069 as compared with 0.080 for the downstream stations. The value of 0.08 for the maximum turbulent intensity is less than that reported by Klebanoff[28], who gives 0.11 from measurements made at U_∞ of 50 ft/sec.

As is seen in Figure 11, the spectral density of the u-fluctuations exhibits good agreement with the measurements of Klebanoff. Figures 11(a) and 11(b) compare spectra

for the inner and outer regions, respectively. In both cases the values of z/δ^* for the pair of Klebanoff curves bracket the z/δ^* value for the present data. None of the u-fluctuation spectral-density curves presented in Figure 11 possesses a well-defined peak for the reported wave numbers.

In Figure 10, the upstream level of free-stream turbulence, 0.012, while high (compared with low-turbulence wind tunnels), is not of concern to the present experiments. The increase in the stream turbulence to about 0.02 at the downstream stations is considered to be a result of the merging of the boundary layers on opposite walls of the wind tunnel. Thus, no correlation measurements and only a limited number of measurements of turbulent intensity and wall-pressure fluctuations were made in this down-stream region, since measurements were to be representative of a turbulent boundary layer developing along a plane wall.

3.2 Magnitude and Spectra of Wall-Pressure Fluctuations

The wall-pressure fluctuations were measured with both types of transducers. Two different types of pressure transducers were used to determine if any of the results were a function of transducer type. In particular, here we consider measurements taken with transducers ZR and CA (see Table I for characteristics of transducers and alphabetic designations). The value of δ^* varied from 0.047 to 0.321 inch for the measurements. The magnitudes $\sqrt{\left(\overline{p_w^2}\right)}$ were obtained from integrating the spectral values that had been corrected for amplitude response of the transducer. If the magnitudes of the wall-pressure fluctuations expressed as $\sqrt{\left(\overline{p_w^2}\right)}\Big/q_\infty$ are plotted with Willmarth's data[19], the result is Figure 12. In this Figure the abscissa d/δ^* is plotted on a log scale to allow the data taken with the smaller transducer ZR to be compared properly not only with Willmarth's data, but also with those of the larger transducer CA . Through Willmarth's data is the line with which he extrapolated to $d/\delta^* = 0$ (on a linear d/δ^* scale) to obtain his result of $\sqrt{\left(\overline{p_w^2}\right)}\Big/q_\infty = 0.006$. Two significant points can readily be made from the Figure: (i) the present data do not agree with Willmarth's data in magnitude, and (ii) the results with the two different types of transducers behave with regard to their variation with d/δ^* almost as if they had been taken with one transducer. If the data for downstream stations x , where $\delta^* > 0.251$ inch (tailed symbols) , are disregarded for reasons previously discussed in Section 3.1, then the scatter of the data is considerably reduced. The remaining values of $\sqrt{\left(\overline{p_w^2}\right)}\Big/q_\infty$ extrapolated to $d/\delta^* = 0$ (again, on a linear scale) yield a value of 0.0075. It is of interest to note that, for a turbulent pipe flow, the work described in Reference 21 obtained a value of 0.008, corrected to zero transducer size by a method described in Reference 29. Lilley and Hodgson[16] quote in their text a value of 0.008 for $d/\delta^* = 0.59$ from their measurement of the boundary layer on the wall of a wind tunnel.

In Figure 13 the spectra of the wall-pressure fluctuations over the range of δ^* from 0.047 to 0.251 inch are plotted in terms of the dimensionless parameters used by Willmarth (see also Ref.18). The dimensionless mean-square spectra are plotted against the dimensionless frequency, a parameter of the character of a Strouhal number if a discrete eddy of a certain size is associated with a given frequency. In Figure 13(a) the data taken with transducer ZR almost completely coincide for different δ^* . In Figure 13(b) for transducer CA a similar degree of coincidence

exists at the lowest and middle frequencies, as in Figure 13(a); but, in addition, at the high-frequency end an effect of the parameter d/δ^* exists that spreads out the data. In Figure 13 each spectrum exhibits a maximum (designated as the relative peak of the spectrum) for values of $(\omega\delta^*)/U_\infty$ between 0.1 and 1.0. However, as smaller values of $(\omega\delta^*)/U_\infty$ are approached, the spectrum again increases to the limit of the available data (this maximum is designated as the absolute peak). Initially it was assumed that, despite the care with which the measurements were made, the existence of the absolute peak was due to some sources of error possibly being overlooked.

The first possibility that quickly suggests itself is that the control block did not successfully perform its function to prevent extraneous noises from propagating upstream into the test section. The results of Figure 14 clearly indicate that this did not occur. Figure 14 gives the results of wall-pressure-fluctuation measurements, at one station, used for determining the effect of varying the longitudinal static-pressure gradient and also the flow conditions at the control block. There is evidence of rather large amplitudes at the low frequencies only when the flow across the control block was allowed to become definitely unchoked. In this case there is a rather large increase in the spectral value, the maximum increase occurring at a frequency of 40 cycles/sec and being from 0.013 to about 0.52 (a factor of 4).

The possibility that fairly large amplitude low-frequency noises were propagating into the test-section from the flow entering the inlet can be ascertained by looking at the results of Figure 15, in which the spectra of the wall-pressure fluctuations (taken with transducer CA) are compared with the external-noise-level spectra just upstream of the wind-tunnel inlet. In the Figure the pressure fluctuations are given in terms of decibels of SPL (sound pressure level, defined as equal to $20 \log_{10}\sqrt{\left(\overline{p^2}/p_0\right)}$, where p_0 is a reference pressure, usually 2×10^{-4} dynes/cm^2). There is no evidence here, also, that the inlet noise is a problem. In fact, at any given frequency the inlet noise levels are 15 decibels or more below the spectra levels of the wall-pressure fluctuations.

In Figure 16 the dimensionless mean-square spectra of the present measurements with transducer ZR are compared with Willmarth's data[18], which show the effect of transducer size on the measured spectra. This behavior is similar to that seen in Figure 13(b) for the larger diameter transducer CA . However, for Willmarth's data the rate of decrease of the spectra with increasing $\omega\delta^*/U_\infty$ at the higher frequency end is greater than that obtained in the present experiments. This may be seen by noting that Willmarth's curve for $d/\delta^* = 1.1$ in Figure 16 agrees with the present data curve for $d/\delta^* = 1.7$ in Figure 13(b). At the lower frequency end of the spectrum Willmarth does not present any data below $\omega\delta^*/U_\infty = 0.1$. Although no mention was made of any problems with extraneous noises that might have interfered with the measurements of the wall-pressure fluctuations, in his dimensionless spectra plot Willmarth included no points for frequencies lower than 1000 cycles/sec.

3.3 Theory and Experiment Compared

If one considers the complete equations of motion and equation of continuity for an incompressible fluid (see Ref. 30), then certain expressions can be obtained for $\overline{p^2(\underline{x},t)}$, the mean-square of the fluctuating pressure, and $\overline{p(\underline{x}_1,t)p(\underline{x}_2,t+\tau)}$, the mean-square pressure covariance. As indicated in References 15 and 16, these

quantities describing the fluctuating pressures depend on second-order, third-order and fourth-order covariances of the fluctuating velocities. The theoretical papers (Refs.15, 16 and 17) have all assumed the terms with the third-order and fourth-order covariances to be negligible compared with the terms involving second-order covariances. In addition, for turbulent-boundary-layer flows the realistic assumption is made that $\partial U_1/\partial x_3$ is much greater than the other mean flow gradients. Consequently, the most significant term is considered to be

$$2 \frac{\partial U_1'}{\partial x_3'} \frac{\partial U_1''}{\partial x_3''} \overline{\frac{\partial u_3'}{\partial x_1'} \frac{\partial u_3''}{\partial x_1''}} .$$

Only this term has been used to calculate the spectrum and magnitude of the mean-square pressure fluctuations and also their space-time correlations. In particular, Lilley, in his theoretical treatment[17], assumes that only the portion of the layer nearest the wall contributes to the pressure fluctuations.

The root-mean-square wall-pressure fluctuations may be expressed, as in Reference 16, as

$$\frac{\sqrt{\left(\overline{p_w^2}\right)}}{q_\infty} = \beta c_f \qquad (1)$$

where the value of β depends upon integration over the turbulent field.

Comparison of the present experimental data with Lilley's theory[17] is given in Figure 17, where $\beta \equiv \sqrt{\left(\overline{p_w^2}\right)}(q_\infty c_f)$ is plotted as a function of d/δ^* to allow comparison with the two transducers. Lilley's theoretical result[17] for the value of β is 3.1 and here appears as a straight line of zero slope, since his theory does not account for the effect of nonzero transducer size. If the experimental data taken with the transducer ZR can be assumed to be correct, there is a small area of disagreement between the experimental and theoretical results in that the experimental results exhibit nonzero slopes, approximately drawn in the Figure. For the very small values of d/δ^*, where no appreciable transducer-size effect should be expected, the values of β are larger than the theoretical value of 3.1. A replot of the data for the smaller transducer ZR on a linear scale for d/δ^* indicates that, as $d/\delta^* \rightarrow 0$, β approaches approximately 3.9. Lilley and Hodgson[16] also quote in their text a value of $\beta = 3.6$ following from their own experiments.

These considerations show that a complete comparison of the experimental and theoretical results would in principle require a more accurate theory. Thus, while the agreement between experiment and theory for the value of β is generally good, the greater value of 3.9 for the experimental value as compared with the theoretical value of 3.1 results from some differences between the present experiments and the assumed models for the mean shear and the fluctuating-velocity spectrum and magnitude.

In certain regions of the turbulent boundary-layer or under certain types of external conditions, the terms neglected in calculations of fluctuating wall-pressures may become of the same order as the term that is kept. An example of this possibility is in the outer or intermittent region where $|\partial U_1/\partial x_3|$ is considerably smaller than in the inner region of the layer.

A comparison of the mean-square spectra for the present data with the Lilley-Hodgson theoretical result[16] is also given in Figure 16. The theoretical curve is taken from Figure 4 of Reference 16 without adjusting the level of the curve. The level of the peak of the theoretical curve is in good agreement with the present experimental data. Very little agreement exists between the present experimental data and this theoretical curve at both ends of the spectrum. This disagreement between the theoretical curve and the experiment should be expected when the velocity spectra upon which they are based are considered. The isotropic form of the velocity correlation function was used in evaluating the theoretical spectrum. Also, an anisotropy factor was used only in evaluating the magnitude of the pressure fluctuations (as previously done by Kraichnan[15]).

The spectra of wall-pressure fluctuations measured in Reference 21 for a turbulent pipe flow also exhibit no fall-off at low frequencies for dimensionless frequencies down to a value of 0.0175, based on the radius of the pipe. However, for the spectra presented there is no indication of the double maxima. The turbulent pipe flow differs from that in the turbulent boundary layer in at least one significant aspect. For pipe flow the absence of a free-stream flow for the region away from the wall precludes the formation of a highly intermittent flow that is brought about by the convection of an irregular sharply defined boundary between the turbulent and the nonturbulent flow (see Ref. 31).

3.4 Space-Time Correlation of Wall-Pressure Fluctuations

The first bit of information obtained from measurements of the space-time correlations of wall-pressure fluctuations was a curve of the correlation coefficient:

$$R(\xi,\eta,\tau) = \frac{\overline{p(x_1,y_1,t)p(x_1+\xi,y_1+\eta,t+\tau)}}{\sqrt{\left\{\overline{p^2(x_1,y_1,t)}\right\}}\sqrt{\left\{\overline{p^2(x_1+\xi,y_1+\eta,t+\tau)}\right\}}} \tag{2}$$

against the time delay τ for constant values of ξ and η. The separation distances are $\xi = x_2 - x_1$ and $\eta = y_2 - y_1$. In equation (2) any point on the curve of $R(\xi,\eta,\tau)$ against τ gives the time-mean value (in coefficient form) of two fluctuating pressures where during the time-averaging the one fluctuating pressure is measured at a constant difference in time equal to τ with respect to the other fluctuating pressure. The results of this section are all obtained from these correlation curves. The two-point wall-pressure correlation curves as a function of τ are presented in Figure 18(a) for $\eta = 0$. The time delay τ is defined to be positive for a disturbance propagating downstream from one transducer to another (farther downstream). These curves are actual tracings of faired X-Y plotter curves. Figure 18(b) is for the case where the transducer separation is given by $\xi = \eta$. The curves in Figure 18(c) are for the correlations with the transducer separation vector normal to the stream direction.

Each point of the results shown in Figure 19 is obtained by first getting the maximum value of the correlation coefficient as a function of τ for fixed separation distance in Figure 18 and then plotting this maximum against the appropriate separation distance. This value of R has been designated by the subscript opt, standing for optimum in Reference 32. The data in Figure 19 include all three inclinations of the transducer separation vectors with the free-stream direction ($\eta = 0$, $\xi = \eta$, and $\xi = 0$).

In looking at Figure 19 it is readily apparent that the longitudinal scale of the wall-pressure fluctuations is much greater than the lateral scale. For example, if scales L_{p_x} and L_{p_y} are arbitrarily defined as the value of the particular separation distance when $R(\xi,0,\tau_{opt}) = 0.1$ and $R(0,\eta,\tau_{opt}) = 0.1$, respectively, the result is

$$\frac{L_{p_x}}{L_{p_y}} = \frac{8.75 \text{ in.}}{1.18 \text{ in.}} \approx 7.4 .$$

In this result the values of τ_{opt} for L_{p_x} and L_{p_y} are not the same in magnitude. For L_{p_x}, $\tau_{opt} = 1.33 \times 10^{-3}$ second and, for L_{p_y}, since no flow convection is involved, $\tau_{opt} \approx 0$. Scale L_{p_x} indicates the scale of the turbulence measured in a reference frame moving at the average convection velocity ξ/τ_{opt}. (If the two pressure transducers at the wall were moving in the direction of flow at this convection velocity, the optimum time delay would be close to zero for the ξ-direction as well as for the η-direction.)

The validity of the empirical relation

$$R_{opt}(\xi,\eta,\tau_{opt_{\xi,\eta}}) = R_{opt}(\xi,0,\tau_{opt_\xi})R_{opt}(0,\eta,\tau_{opt_\eta}) \qquad (3)$$

where

$$\tau_{opt_\xi} \approx \tau_{opt_{\xi,\eta}}$$

and

$$\tau_{opt_\eta} \approx 0$$

is shown in Figure 20, where it is checked for $\xi = \eta$. This was done by using the curves faired through the data in Figures 19(a) and (c) to obtain the calculated curve for the left side of equation (3) and then comparing it with the curve faired through the data of Figure 19(b). The agreement between the two curves in Figure 20 is quite good. The result should also be valid for $\xi \neq \eta$. The result expressed by equation (3) was first implied by the correlation data on fluctuating velocities in a turbulent boundary layer in Reference 32. Equation (3) was later assumed by Corcos et alii[29] in their calculation on the effects of finite sizes of pressure transducers.

In Figure 21 the optimum correlation coefficients in the ξ-direction are compared with those measured by Willmarth. The values ξ are divided by δ^* to account for the differing scales in the two sets of data. The agreement between the present data and thoseof Willmarth is good, particularly for his data for $M = 0.333$ and $M = 0.672$.

The value of τ at which $R \equiv R_{opt}$ is likewise designated as τ_{opt}. In Figure 18(a) it is seen that τ_{opt} increases as ξ is increased. The convection velocity of the wall-pressure fluctuations is defined as

$$U_c = \frac{\xi}{\tau_{opt}} \qquad (4a)$$

and the ratio of the convection velocity to the free-stream velocity is simply

$$\frac{U_c}{U_\infty} = \frac{\xi}{\tau_{opt} U_\infty} .$$

These values of U_c/U_∞ were plotted against the appropriate separation distance in Figures 22(a) and (b) for $\eta = 0$ and $\xi = \eta$, respectively. For $\xi < 1.0$ inch in Figure 22(a), U_c/U_∞ increases at a smaller rate with increasing ξ. In Figure 22(b), at values of $\xi > 1.0$ inch the values of U_c/U_∞ start to fall with increasing ξ. A check of the R against τ curves for these points shows very small values of R_{opt} and very flat curves. Consequently, not too much reliance should be put on the data at large ξ.

The convection velocity results given in Figure 22 are quite interesting in that at large values of ξ they essentially agree with the convection velocity values obtained by Willmarth[19] (excepting his $M = 0.672$ data) and Von Winkle[21]. At the smaller values of ξ the convection velocity ratio U_c/U_∞ begins to decrease significantly as ξ is decreased. This result can reasonably be interpreted if one considers the decay and convection of the different size eddies that probably exist in the boundary layer. The smaller scale eddies should have a shorter lifetime compared with the larger scale eddies. Consequently, as the separation distance between the two pressure transducers is increased, the effect of the smaller scale eddies on the correlation of the pressure fluctuations measured by these transducers should decrease with the correlation, being affected only by the large-scale eddies in the boundary layer. Finally, the small-scale eddies occur or are concentrated closer to the wall than are the large-scale eddies. Thus, the small-scale eddies are convected at slower velocities than are the large-scale eddies. This simplified picture is proposed to describe the results of Figure 22 for small values of ξ.

This interpretation of the Figure 22 data implies that the value of U_c/U_∞ should decrease with increasing frequency. Correlation of the data in narrow frequency bands was not done with the present data. However, the results of Reference 21 for turbulent pipe flow indicate such a trend. Figure 36 of Reference 21 shows that, as the frequency increases by a factor of 2.8, the values of U_c/U_∞ decrease from 0.83 to 0.75.

A comparison of the U_c/U_∞ data with Willmarth's results is presented in Figure 23. To take into account the range in the values of U_∞ and δ^*, the U_c/U_∞ values are given as a function of $U_\infty(\xi/\delta^*)$. Initially, the dimensional parameter U_∞/ξ was considered. Dividing ξ by δ^* does account for the different length scales. A suitable velocity is not available (the acoustic velocity not being appropriate here) with which to make the entire parameter dimensionless. However, this choice of parameters should account for the different velocity and length scales. The comparison of the U_c/U_∞ data does show that the scatter in the data is nearly the same and the agreement is good. The limited range of the $U_\infty/(\xi/\delta^*)$ parameter for the Willmarth data as compared with the present data simply results from the smaller range of ξ for which measurements were made by Willmarth. The abscissa positions of the Willmarth data relative to the present data show why smaller values of U_c/U_∞ could not be obtained in his experiment. The results in Figure 23 indicate that in addition to considering the size of the transducers relative to a boundary-layer scale as noted by Willmarth[19] it is necessary to consider very small separation distances ξ (relative to some boundary-layer scale such as δ^*) when convection velocities of pressure fluctuations are to be determined.

Measurements for M_∞ from 2.0 to 5.0 by Laufer and Kistler[33] indicate at least a qualitative agreement with the data in Figure 22. Measurements are reported for only two values of ξ (0.25 and 0.50 in.) with the values of U_c/U_∞ varying between 0.65 and 0.77. At each M_∞ the value of U_c/U_∞ for the larger ξ is greater than that for the smaller ξ with the average increase being about 7 percent.

The preceding discussion indicates that, as expected, the value of the apparent convection velocity depends on the relative magnitudes of (1) transducer size and separation distance and (2) the sizes of the eddies and their velocities of convection in the layer. Therefore, these results apply only to convection velocities of the wall-pressure fluctuations of turbulent boundary layers along a plane wall under the aforementioned conditions of measurement. They may not apply in general where larger size transducers, larger separation distances, or a different type of turbulent flow is involved.

The effect of high-pass filtering (which equals rejection of a low-frequency band of the signals) on typical correlations is given in Figure 24(a) for $\xi = 0.88$ and $\eta = 0$ and in Figure 24(b) for $\xi = 0$ and $\eta = 0.325$ inch. With regard to the present experiments, some concern has been expressed that the large magnitudes of the spectrum of the wall-pressure fluctuations at the lower frequencies may have resulted from some as yet undetermined wind-tunnel effect. Since this increase in the magnitudes occurs approximately at frequencies below 400 cycles/sec, a comparison of the correlation data for the full bandwidth spectrum with those for which the portion of the spectrum below 400 cycles/sec is rejected would indicate how significant is this lower frequency range on the space-time correlations. It is seen in Figures 24(a) and (b) that rejecting the portion of the spectrum below 400 cycles/sec results in optimum correlation coefficients that do not change appreciably from those for the entire spectrum. In particular, for the 400 cycles/sec high-pass condition, the R_{opt} are approximately only 10 percent less than those for the full-band-pass results.

3.5 Correlations of Velocity and Wall-Pressure Fluctuations

Investigations on the correlations of pressure with velocity in turbulent flow fields have generally not been attempted either on an experimental or theoretical basis. Reference 34 does give some numerical results for the covariances $\overline{pu_k^2}$ for isotropic turbulence. The role of the pressure-velocity-gradient covariance $\overline{p(\partial u_k/\partial x_i)}$ is discussed in Reference 35. The particular form of the pressure-velocity covariance of interest herein is $\overline{pu_k}$. The defining equation for $\overline{pu_k}$ is given by Batchelor[36] as (in the present notation)

$$\overline{pu_k''} = \frac{\rho}{4\pi}\int \frac{1}{|\underline{r}'|}\,\frac{\overline{\partial^2(U_i' + u_i')(U_j' + u_j')(U_k'' + u_k'')}}{\partial x_i'\,\partial x_j'}\,d^3x'$$

(where $|\underline{r}'|$ is the distance between the source point and field point) if an incompressible fluid in an infinite region is assumed. The corresponding correlation coefficient is given by $\overline{pu_k''}$ divided by the product of the root-mean-square wall-pressure and velocity fluctuations.

The purpose behind measuring these correlations is to determine what regions within the boundary layer contribute to the pressure fluctuations at the wall.

Measurements of the pressure fluctuations at one point at the wall or their space-time correlations do not yield any detailed information on what regions do contribute. Actually, a study of the correlations with each of the components of the fluctuating velocity would be desirable. In particular, the theoretical considerations of Reference 16 indicate the w-component to be the most significant one. However, the measurements of v or w, the fluctuating-velocity components normal to the free-stream direction, would require two hot wires in the available experimental set-up. (The method requiring the rotation of one wire could not be used because of the necessity of keeping the hot-wire position fixed relative to the pressure-transducer position for a given measurement, i.e. a single recording on magnetic tape.) Thus, getting a measure of $\overline{pw}$ or $\overline{pv}$ would ordinarily require at least three channels on the tape recorder. As noted previously, the tape recorder and playback units available for use had only two channels.

Typical space-time correlation curves obtained for the correlation of the velocity fluctuations with wall-pressure fluctuations are presented in Figures 25 and 26. The correlation coefficient used in this section is defined by equation (5). The script $\mathcal{R}$ for the velocity-pressure correlation is used here to distinguish it from the space-time correlations of the wall-pressure fluctuations. The definition of positive values of τ for the pressure-velocity correlations is that a disturbance propagating downstream is first sensed by the wall-pressure transducer and at a later time τ is sensed by the hot wire. As for the previous type of correlation measurements, each curve presented in Figures 25 and 26 is a direct tracing of a faired curve of the X-Y plotter curve. In some cases the X-Y plotter curve was retraced several times over the original one to allow a better fairing.

The results given in Figure 25 are for the correlations measured with transducer ZS and for several pairs of values of separation distances η and ξ. Figure 25(a) gives $\mathcal{R}_{opt}$ against τ for several values of z at ξ and η approximately zero. Figures 25(b) and 25(c) give similar results where (ξ, η) are (0, 0.307) and (0.390, 0), respectively. Peaks in the correlation coefficient generally occur at two values of time delay τ. The major peak generally occurs at values of τ ranging between -0.7 and -0.8 millisecond. For purposes of identification, values of τ and $\mathcal{R}$ for the major peaks are labeled with the subscript opt and for the secondary peaks ($\tau < 0$) with the subscript s.

A typical correlation curve for z less than 0.3 inch does not have a secondary peak but, for $\tau < \tau_{opt}$, generally increases monotonically with increasing τ and then decreases monotonically for $\tau > \tau_{opt}$. For values of z greater than 0.3 inch the emergence of $\mathcal{R}_s$ caused most of the $\mathcal{R}$ against τ curves to have two rounded peaks of about the same magnitude at the smaller values of z and, for z between 0.72 to 1.52 inches, resulted in $\mathcal{R}_s$ being greater in magnitude than $\mathcal{R}_{opt}$. In other words, regardless of the value of the separation distance ξ, for positions of the hot wire close to the wall the $\mathcal{R}_{opt}$ is the greater one, but for positions away from the wall $\mathcal{R}_s$ is of the same order or even slightly greater than $\mathcal{R}_{opt}$.

In Figure 26 the correlation curves are given for ξ and η approximately zero, where the transducer CB is used to measure the wall-pressure fluctuations. These results confirm the measurements using transducer ZS; however, the peak values are generally somewhat lower in magnitude. In addition, the curves are not as well behaved as those in Figure 25, as $\mathcal{R}_{opt}$ is approached from negative values of τ.

Significant characteristics of the correlation curves are plotted in Figure 27. These curves include results not presented in the preceding Figures. Figure 27(a) gives the significant characteristics of the correlation curves using transducer ZS for various values of ξ and $\eta \approx 0$. The R_{opt} and R_s data in Figure 27(a) do not indicate a steady trend, as in Figure 27(b). The variation of τ_{opt} with z in Figure 27(a) is such that, at any value of z greater than about 0.1 inch, τ_{opt} increases as ξ is increased. For any value of ξ the variation of τ_{opt} with z is approximately linear if z is greater than 0.2 inch. Over most of the range of z values, τ_s also increases (values become less negative) as ξ is increased (Fig.27(a)). In Figure 27(b) the results are as for their counterparts in Figure 27(a), except that here $\xi \approx 0$ and each figure contains curves for the various values of η. In Figure 27(b) the results of R_{opt} against z are indeed a very regularly behaved set of data in contrast to the data of Figure 27(a). The maximum values of R_{opt} for each curve η = constant are progressively smaller and occur at larger values of z as η is increased. The curves of τ_{opt} as a function of z in Figure 27(b) exhibit a marked change of slope for η greater than about 0.4 inch. For values of z less than 0.4 inch a systematic change also occurs in that larger values of τ_{opt} appear to be reached for η larger as z gets smaller. There is only a slight systematic trend in the maximum values of R_s against z curves with η; the curves of τ_s against z show an overall increase in τ_s with increasing η.

Two possibly serious problems must be considered in trying to make meaningful measurements of the correlation of wall-pressure and velocity fluctuations. One is the fact that the velocity-fluctuation transducer (the hot-wire anemometer) and the pressure-fluctuation transducers are probably not perfectly matched transducers with regard to their phase-angle response as a function of frequency. The necessity to consider not only amplitude response but also the phase-angle response of a transducer over the frequency range of interest arises from the fact that, if two transducers have at a particular frequency two considerably different values of phase-angles φ_1 and φ_2, at that frequency the correlation will be a function of $\cos(\varphi_2 - \varphi_1)$.

Although these phase-angle characteristics were not measured, it can be stated that for the frequency range of interest, 50 to 15,000 cycles/sec, the phase angle as a function of frequency for the piezoelectric transducer shows somewhat less variation than that for the condenser transducer. Since the piezoelectric transducers exhibit less variation over the indicated frequency range than the condenser transducer, elementary considerations of transducer theory show that this will lead to less variation in the phase-angle as a function of frequency[37]. As is seen by comparing Figures 25(a) and 26, there is fair agreement between the correlation curves for the two types of transducers. The most noticeable difference between the two sets of data is that the values of R are slightly lower for the set where the pressure transducer is of the condenser type. This result is consistent with the preceding remarks on the phase-angle characteristics of the two types of pressure transducers. Thus, for these purposes the piezoelectric transducers are more nearly matched to the hot-wire anemometer than are the condenser transducers. If a phase-angle difference does exist between the velocity and pressure transducers used to obtain the correlations, its effect would be to reduce to a certain extent the magnitudes of the correlation coefficients. This implies that ideally matched transducers might yield even larger values of the correlation coefficient than those measured. Consequently, the

magnitudes of the correlation coefficients measured may be regarded as tentative results.

The second major problem encountered in the measurement of the pressure-velocity correlations is the existence of interference between the hot-wire probe and the flow field, as indicated in Figure 28, which presents the spectra of the wall-pressure fluctuations measured during the correlation experiments. The data in these Figures indicate that the shapes of these wall-pressure fluctuation spectra are affected to a certain extent by the proximity of the hot-wire probe. The spectra in Figures 28(a) to 28(d) are taken with transducer ZS for $\eta \approx 0$ and various values of ξ. In Figure 28(a) with ξ = -0.001 inch, that is with the hot wire directly above the pressure transducer, the spectra values below 400 cycles/sec increase in magnitude as the z values get smaller.

The effect of moving the hot-wire probe downstream away from the pressure transducer is noted by comparing Figures 28(a) to 28(d) with each other. Virtually no increase in the value of F(f) is obtained for the frequencies lower than about 400 cycles/sec as the value of z is allowed to decrease. Similar results were noted for the interference of the hot-wire probe on the wall-pressure fluctuations where the displacements in the plane of the wall are in a direction normal to the free-stream.

From results such as those presented in Figure 28 it is noted that only the magnitudes of the lower frequency portion of the spectrum of the wall-pressure fluctuations are increased as z is allowed to decrease for ξ and η approximately less than 0.20 inch. Consequently, one may omit from serious consideration those correlations for smaller values of z(< 0.20 in.) when ξ and η are less than approximately 0.20 inch. On the other hand, all the data may be considered if one observes the effects of filtering out the lower frequency portion of the spectrum, which is apparently most affected by the interference. Figure 29 presents the effect of using only a certain portion of the spectrum in the correlations of the velocity fluctuations with the wall-pressure fluctuations. The correlation curves are the full band pass and 400 cycles/sec, 3000 cycles/sec and 6000 cycles/sec high-pass band ($\xi \approx \eta \approx 0$). It is only in the range of frequencies below 400 cycles/sec that the spectra of the wall-pressure fluctuations show any appreciable interference effect from the hot-wire probe. Consequently, the fact of particular interest in Figure 29 is the comparison of the peak correlation coefficient for the full band pass with that for the 400 cycles/sec high-pass band. The values of R_{opt} are 0.60 and 0.52 for the full band pass and 400 cycles/sec high-pass band, respectively. This indicates that the fluctuations below 400 cycles/sec do not contribute appreciably to the correlation coefficients measured. Consequently, this interference effect should not affect the measurements of pressure-velocity correlation. As in the case of the space-time correlations of the wall-pressure fluctuations, the rejection of this lower frequency portion of the spectrum also serves to remove those portions of the spectra that might be affected by wind-tunnel disturbances.

In Figure 29 the correlation curve of R as a function of τ was made considerably narrower when the portion of the spectrum below 400 cycles/sec was filtered out.

In addition to the normal effect of using filters, this narrowing actually might be the result of rejecting those portions of the spectrum affected by interference. In the following only the magnitudes of R and τ at the peaks will be discussed. Considerations of the shapes of the curves will not be particularly stressed.

The results given in Figures 25 to 27 indicate that the u-component of the fluctuating velocity does make some contribution to the pressure fluctuations at the wall. This follows from the fact that nonzero values of R were obtained. The results indicate that there are two regions in the boundary layer where the u-component contributes to the pressure fluctuations at the wall. These are the inner region (close to the wall) and the outer region, which is highly intermittent. While the magnitudes of the R obtained for the inner region (R_{opt}) are higher than those obtained for the outer region (R_s), the amount of actual contribution of these two regions will depend on the volumes in each region over which the R is appreciable.

According to the leading assumptions in the Lilley-Hodgson theory[16] the wall-pressure fluctuations depend significantly only on the w-component of velocity fluctuations for the inner region of the boundary layer. This implies that, in correlating the wall-pressure fluctuations with the velocity fluctuations, larger magnitudes of the correlation coefficients may be obtained with the w-component of velocity fluctuations than with the other two components. As the other components of velocity fluctuations were not measured and were not correlated with the pressure fluctuations, the results between components cannot be compared. However, it is to be noted that any given value of R for the particular ξ, η, z, and τ is the covariance $p_w u$ divided by the product of $\sqrt{(\overline{p_w^2})}$ and $\sqrt{(\overline{u^2})}$. What would be more appropriate is to get a value R' defined as

$$R' = \frac{\sqrt{(\overline{p_w u})}}{\sqrt{(\overline{p_w^2})}\sqrt{(\overline{u^2} + \overline{v^2} + \overline{w^2})}} \tag{6}$$

which is simply

$$R' = R \frac{\sqrt{(\overline{u^2})}}{\sqrt{(\overline{u^2} + \overline{v^2} + \overline{w^2})}} \tag{7}$$

in terms of R, the measured correlation coefficient.

Although no measurements were made of $\overline{v^2}$ and $\overline{w^2}$, values of R' can be computed using Klebanoff's data[28]. For the inner region of the boundary layer it is seen from Figure 27(a) that the measured R_{opt} as a function of z has maximum values approximately at $z = 0.08$ inch, which becomes $z/\delta^* = 0.45$ with $\delta^* = 0.178$ inch. For $z/\delta^* = 0.45$, Klebanoff's data yield the values $\sqrt{(\overline{u^2})} = 0.08$, $\sqrt{(\overline{v^2})} = 0.06$, and $\sqrt{(\overline{w^2})} = 0.035$. Thus,

$$\frac{\sqrt{(\overline{u^2})}}{\sqrt{(\overline{u^2} + \overline{v^2} + \overline{w^2})}} = \frac{0.08}{0.106} = 0.76 . \tag{8}$$

For a measured value of $R = 0.34$ with $\xi \geq 0.20$ inch and $\eta \approx 0$, a value of R' of 0.26 is obtained. It is now evident that, even for the correlation coefficients based on the root mean square of the entire velocity fluctuations, for the inner region significant nonzero values of correlation are obtained between the wall-pressure and u-component of velocity fluctuations. And yet, as previously pointed out, if the theoretical model is correct, the correlations between the pressure and w-component of velocity fluctuations should yield much higher values of correlation coefficients, where R in this case must be defined as

$$R = \frac{\overline{p_w w}}{\sqrt{\left(\overline{p_w^2}\right)}\sqrt{\left(\overline{w^2}\right)}} . \tag{9}$$

In the curves of R against τ the peak correlation coefficients designated as R_s attain maximum values for z values that are much larger than those for the R_{opt} values already discussed. (The 'secondary' peaks R_s are those peaks occurring at negative time delays of nearly 1 msec in contrast to the R_{opt} peaks which occur at positive time delays near zero.) The initial reaction in viewing these R_s peaks for the preliminary results was that they were erroneous. The entire system of measurement and correlation was thoroughly checked. These peaks were not found to be the result of some problem of instrumentation or measurement such as the interference effect of the hot-wire probe. For this range of z the interference effect of the hot-wire probe was negligible for all values of separation distances ξ and η.

Since this result is limited to the outer region of the boundary layer, the intermittency that also exists in this region is considered to be quite significant. In Figure 30 the data of Klebanoff[28] and Corrsin and Kistler[31] for the intermittency factor γ are compared with R_s as a function of z/δ^* for several surveys. For Klebanoff's data, originally given as a function of z/δ^*, his mean-velocity data were used to calculate δ/δ^* to obtain γ as a function of z/δ^*. Because the Corrsin-Kistler experiments used a corrugated wall, the calculation of δ^* from the mean-velocity profile was considered unwise in this case. Since both Klebanoff and Corrsin-Kistler gave γ as a function of z/δ, the method of converting γ into a function of z/δ^* was first to compare the Klebanoff and Corrsin-Kistler data at a particular value of z/δ and then to use the Klebanoff z/δ^* to plot the value of γ for the Corosin-Kistler data.

In Figure 30 the maximum values of R_s occur in the intermittent region of the layer as defined by γ as a function of z/δ^*. Particularly good agreement seems to exist with the intermittent region as defined by the Corrsin-Kistler data. Their data compared with the Klebanoff data show a stronger penetration of the intermittent fluctuations at distances greater than δ. The agreement between R_s and γ is tempered by the fact that nonzero values of R_s extend out to larger values of z/δ^* than do the nonzero values of γ for either the Klebanoff or Corrsin-Kistler data. While the intermittency factor γ was not measured in the present investigation, the turbulent intensities for the outer region of the boundary layer are greater and extend further from the wall compared with the Klebanoff or the Corrsin-Kistler data. As previously remarked, the magnitudes of these R_s values are approximately one-half the R_{opt} values obtained in the inner region. Furthermore, if again R'

is calculated by using Klebanoff's data, which show that for the outer region $\sqrt{(\overline{u^2})} \approx \sqrt{(\overline{v^2})} \approx \sqrt{(\overline{w^2})}$, there is obtained

$$R' = R \frac{\sqrt{(\overline{u^2})}}{\sqrt{(\overline{u^2} + \overline{v^2} + \overline{w^2})}} = 0.57R .$$

This implies that, although the u-component fluctuations in the outer region contribute to the wall-pressure fluctuations, the magnitude of the contribution from a particular point is not as great as that from the inner region.

For most of the values of ξ and η, the time delays τ_{opt} generally increase with increasing z. Attempts at trying to relate the τ_{opt} values to the convection velocities measured in the space-time correlations of wall-pressure fluctuations have not been successful using the present data.

The negative values obtained for the time delays denoted as τ_s in Figures 27(a) and 27(b) indicate a behavior of the correlation of the velocities with the wall-pressure fluctuations different from that for the inner region (R_{opt} and τ_{opt}). These negative τ_s values require that even for $\xi \equiv 0$ the velocity fluctuations that correlate with the wall-pressure fluctuations must occur some distance upstream of the pressure transducer and hot-wire probe. This is interesting in that it agrees with the results of Reference 38. This reference shows (in Fig. 4 therein) results that indicate that the u-component of the fluctuating velocities does have an effective eddy convection velocity in the z-direction, but that it is considerably less than that for the free-stream direction. These results imply that the large-scale velocity fluctuations in the outer region that eventually affect the pressure at the wall must originate a considerable distance upstream in order for the slower convection in the z-direction to have sufficient time to reach the wall. Rough calculations of τ_s based on the results of Reference 38 give values from -0.45×10^{-3} to -0.6×10^{-3} second, whereas the present results range from -0.7×10^{-3} to -0.8×10^{-3} second. However, it is not suggested that this simple concept sufficiently explains the phenomenon.

4. CONCLUSIONS

The following conclusions may be drawn from this experimental investigation of the wall-pressure fluctuations in a turbulent boundary layer:

(i) The value of the root-mean-square wall-pressure fluctuations approaches $\sqrt{(\overline{p^2})} = 0.0075\, q_\infty$ as d/δ^* approaches zero (where q_∞ is the free-stream mean dynamic pressure, d is the diameter of the pressure transducer, and δ^* is the displacement thickness of the boundary layer).

(ii) The measured values of β in the relation $\sqrt{(\overline{p^2})}/q_\infty = \beta c_f$ (where c_f is the local skin-friction coefficient) depend on d/δ^*. By extrapolating the measured β to $d/\delta^* = 0$, there results $\beta = 3.9$, which is in good agreement but slightly higher than the value of 3.1 obtained from the most recent Lilley analysis[17].

(iii) As the transducer size is decreased, the dimensionless mean-square spectrum $[\Phi(\omega)U_\infty]/(q_\infty^2\delta^*)$ of the wall-pressure fluctuations apparently approaches a universal function of the dimensionless frequency $\omega\delta^*/U_\infty$ as indicated by Willmarth for the upper range of $\omega\delta^*/U_\infty$, but this universal function agrees with the data obtained by Willmarth only for his lowest reported values of $\omega\delta^*/U_\infty$.

(iv) The dimensionless mean-square spectrum of the wall-pressure fluctuations as a function of the dimensionless frequency $\omega\delta^*/U_\infty$ does not agree with the Lilley-Hodgson theoretical result[16], except near the peak of the theoretical spectrum.

(v) The values of the correlation coefficients R_{opt} as a function of ξ/δ^* (the longitudinal separation distance divided by the boundary-layer displacement thickness) agree with those obtained by Willmarth.

(vi) Measurements of the correlation coefficients R_{opt} in the lateral direction η indicate that their scale is 1/7.4 of those obtained for the R_{opt} in the longitudinal direction ξ.

(vii) Measurements indicate that for any ξ and η separation the R_{opt} can be obtained from the relation $R_{opt}(\xi,\eta,\tau_{opt}) = R_{opt}(\xi,0,\tau_{opt})R_{opt}(0,\eta,\tau_{opt})$.

(viii) The ratio of the convection velocity to the free-stream velocity U_c/U_∞ is shown not to be a constant but to increase with increasing separation distance ξ and for the larger separation distances to agree with the values obtained by Willmarth. This variation in the magnitude of the convection velocity is explained in terms of the relative distances in which the small-scale and large-scale eddies are coherent.

(ix) Correlations of the wall-pressure fluctuations with the longitudinal component of the velocity fluctuations indicate that the contributions to the wall-pressure fluctuations are associated with two regions - an inner region near the wall and an outer region linked with the intermittency near the edge of the boundary layer. In the outer region the intensity of the contributions of the velocity fluctuations to the wall-pressure fluctuations as indicated by the magnitude of the correlation coefficients is less than one-half that for the inner region.

5. CONCLUDING REMARKS

In the previous section several definite conclusions have been stated. Some further remarks on the results can be made:

(i) To lessen the disagreement between the available theoretical analyses and the available experiments on the spectra of the wall-pressure fluctuations probably requires that less simplified assumptions be used in the theoretical work. Some additional experimental work should be performed to corroborate the results of this investigation, particularly for values of dimensionless frequency $\omega\delta^*/U_\infty$ smaller than 0.07.

(ii) The results obtained for the correlations of the u-component of velocity fluctuations with the wall-pressure fluctuations definitely suggest that experiments be performed to study the intensity and extent of the correlations where the other two components of velocity fluctuations are used. Since the theoretical models for the problem suggest that the w-component of the velocity fluctuations is the dominant one in contributing to the wall-pressure fluctuations, correlation coefficients of greater magnitude should be obtained for the correlations with the w-components than those with the u-components. More elaborate facilities than those used herein would be required for these measurements.

ACKNOWLEDGEMENTS

Acknowledgement is made to Dr. Gustav Kuerti of the Case Institute of Technology for his interest and advice in the preparation of this work.

REFERENCES

1. Lighthill, M.J. — *On Sound Generated Aerodynamically. I - General Theory.* Proc. Roy Soc. (London), Ser. A, Vol. 211, No. 1107, Mar. 20, 1952, pp. 564-587.

2. Lighthill, M.J. — *On Sound Generated Aerodynamically. II - Turbulence as a Source of Sound.* Proc. Roy. Soc. (London), Ser. A, Vol. 222, No. 1148, Feb. 23, 1954, pp. 1-32.

3. Ribner, H.S. — *A Theory of the Sound from Jets and Other Flows in Terms of Simple Sources.* Rep. 67, Inst. Aerophys., Univ. Toronto, July 1960.

4. Proudman, I. — *The Generation of Noise by Isotropic Turbulence.* Proc. Roy. Soc. (London), Ser. A, Vol. 214, No. 1116, Aug. 7, 1952, pp. 119-132.

5. Mawardi, Osman K. — *On the Spectrum of Noise from Turbulence.* Jour. Acoustical Soc. Am., Vol. 27, No. 3, May 1955, pp. 442-445.

6. Meecham, W.C. Ford, G.W. — *Acoustic Radiation from Isotropic Turbulence.* Jour. Acoustical Soc. Am., Vol. 30, No. 4, Apr. 1958, pp. 318-322.

7. Curle, N. — *The Influence of Solid Boundaries Upon Aerodynamic Sound.* Proc. Roy. Soc. (London), Ser. A, Vol. 231, No. 1187, Sept. 20, 1955, pp. 505-513.

8. Phillips, O.M. — *On the Aerodynamic Surface Sound from a Plane Turbulent Boundary Layer.* Proc. Roy. Soc. (London), Ser. A, Vol. 234, No. 1198, Feb. 21, 1956, pp. 327-335.

9. Doak, P.E. — *Acoustic Radiation from a Turbulent Fluid Containing Foreign Bodies.* Proc. Roy. Soc. (London), Ser. A, Vol. 254, No. 1276, Jan. 19, 1960, pp. 129-145.

10. Powell, Alan — *On the Aerodynamic Noise of a Rigid Flat Plate Moving at Zero Incidence.* Jour. Acoustical Soc. Am., Vol. 31, No. 12, Dec. 1959, pp. 1649-1653.

11. Powell, Alan — *Aerodynamic Noise and the Plane Boundary.* Jour. Acoustical Soc. Am., Vol. 32, No. 8, Aug. 1960, pp. 982-990.

12. Heisenberg, W. — *Zur statistischen Theorie der Turbulenz.* Zs. f. Phys., Bd. 124, Heft 7/12, 1948, pp. 628-657.

13. Batchelor, G.K. — *Pressure Fluctuations in Isotropic Turbulence.* Proc. Cambridge Phil. Soc. Pt. 2, Vol. 47, Apr. 1951, pp 359-374.

14. Kraichnan, Robert H. — *Pressure Field Within Homogeneous Anisotropic Turbulence.* Jour. Acoustical Soc. Am., Vol. 28, No. 1, Jan. 1956, pp. 64-72.

15. Kraichnan, Robert H. — *Pressure Fluctuations in Turbulent Flow over a Flat Plate.* Jour. Acoustical Soc. Am., Vol. 28, No. 3, May 1956, pp. 378-390.

16. Lilley, G.M. Hodgson, T.H. — *On Surface Pressure Fluctuations in Turbulent Boundary Layers.* AGARD Rep. 276, Apr. 1960.

17. Lilley, G.M. — *Pressure Fluctuations in an Incompressible Turbulent Boundary Layer.* Rep. 133, The College of Aero. (Cranfield), June 1960.

18. Harrison, Mark — *Pressure Fluctuations on the Wall Adjacent to a Turbulent Boundary Layer.* Rep. 1260, David Taylor Model Basin, U.S.A., Dec. 1958.

19. Willmarth, W.W. — *Space-Time Correlations and Spectra of Wall Pressure in a Turbulent Boundary Layer.* NASA MEMO 3-17-59W, 1959.

20. Skudrzyk, E.J. Haddle, G.P. — *Noise Production in a Turbulent Boundary Layer by Smooth and Rough Surfaces.* Jour. Acoustical Soc. Am., Vol. 32, No. 1, Jan. 1960, pp. 19-34.

21. Von Winkle, William A. — *Some Measurements of Longitudinal Space-Time Correlations of Wall Pressure Fluctuations in Turbulent Pipe Flow.* Inst. Eng. Res., Univ. Calif., Sept. 1961.

22. Serafini, John S. — *Wall-Pressure Fluctuations in a Turbulent Boundary Layer.* Ph.D. Thesis, Case Inst. Tech., 1962. (Also proposed NASA Rep., 1963.)

23. Ludwieg, H.; Tillmann, W. — *Investigations of the Wall-Shearing Stress in Turbulent Boundary Layers.* NACA TM 1285, 1950.

24. Laurence, James C.; Landes, L. Gene — *Auxiliary Equipment and Techniques for Adapting the Constant-Temperature Hot-Wire Anemometer to Specific Problems in Air-Flow Measurements.* NACA TN 2843, 1952.

25. Laurence, James C. — *Intensity, Scale, and Spectra of Turbulence in Mixing Region of Free Subsonic Jet.* NACA Rep. 1292, 1956. (Supersedes NACA TN 3561 and TN 3576.)

26. Sandborn, Virgil A. — *Experimental Evaluation of Momentum Terms in Turbulent Pipe Flow.* NACA TN 3266, 1955.

27. Schlichting, Hermann — *Boundary Layer Theory.* McGraw-Hill, 1955.

28. Klebanoff, P.S. — *Characteristics of Turbulence in a Boundary Layer with Zero Pressure Gradient.* NACA Rep. 1247, 1955. (Supersedes NACA TN 3178.)

29. Corcos, G.M. et alii — *On the Measurement of Turbulent Pressure Fluctuations with a Transducer of Finite Size.* Inst. Res. Eng., Univ. Calif., 1959.

30. Townsend, A.A. — *The Structure of Turbulent Shear Flow.* Cambridge Univ. Press, 1956, p. 27.

31. Corrsin, Stanley; Kistler, Alan L. — *Free-Stream Boundaries of Turbulent Flows.* NACA Rep. 1244, 1955. (Supersedes NACA TN 3133.)

32. Favre, A.J. et alii — *Space-Time Double Correlations and Spectra in a Turbulent Boundary Layer.* Jour. Fluid Mech., Pt. 4, Vol. 2, June 1957, pp. 313-342.

33. Richards, E.J. et alii — *Boundary Layer Noise Research in the U.S.A. and Canada: A Critical Review.* Rep. 21,766, ARC, Gt. Britain, Feb. 1960.

34. Limber, D.N. — *Numerical Results for Pressure-Velocity Correlations in Homogeneous Isotropic Turbulence.* Proc. Nat. Acad. Sci., Vol. 37, 1951, p. 230.

35. Hinze, J.O. — *Turbulence.* McGraw-Hill, 1959, p. 252.

36. Batchelor, G.K. — *The Theory of Homogeneous Turbulence.* Cambridge Univ. Press, 1956.

37. MacColl, LeRoy A. *Fundamental Theory of Servomechanisms.* D. Van Nostrand, 1945.

38. Favre, A.J. et alii *Further Space-Time Correlations of Velocity in a Turbulent Boundary Layer.* Jour. Fluid Mech., Pt. 4, Vol. 3, Jan. 1958, pp. 344-356.

TABLE I

List of Pressure Transducers

Type of transducer	*Diameter of sensing area (in.)*	*Commercial designation*	*Alphabetic designation*	*Type of surface of sensitive area (adjacent to flow)*
Condenser	0.43	Altec-Lansing BR 150-5	CA	Porous bronze
Condenser	0.040	Altec-Lansing BR 150-6	CB	Open pin-hole
Piezoelectric	0.0625	-	ZR	Polished insulating end cap
	0.125	-	ZS	

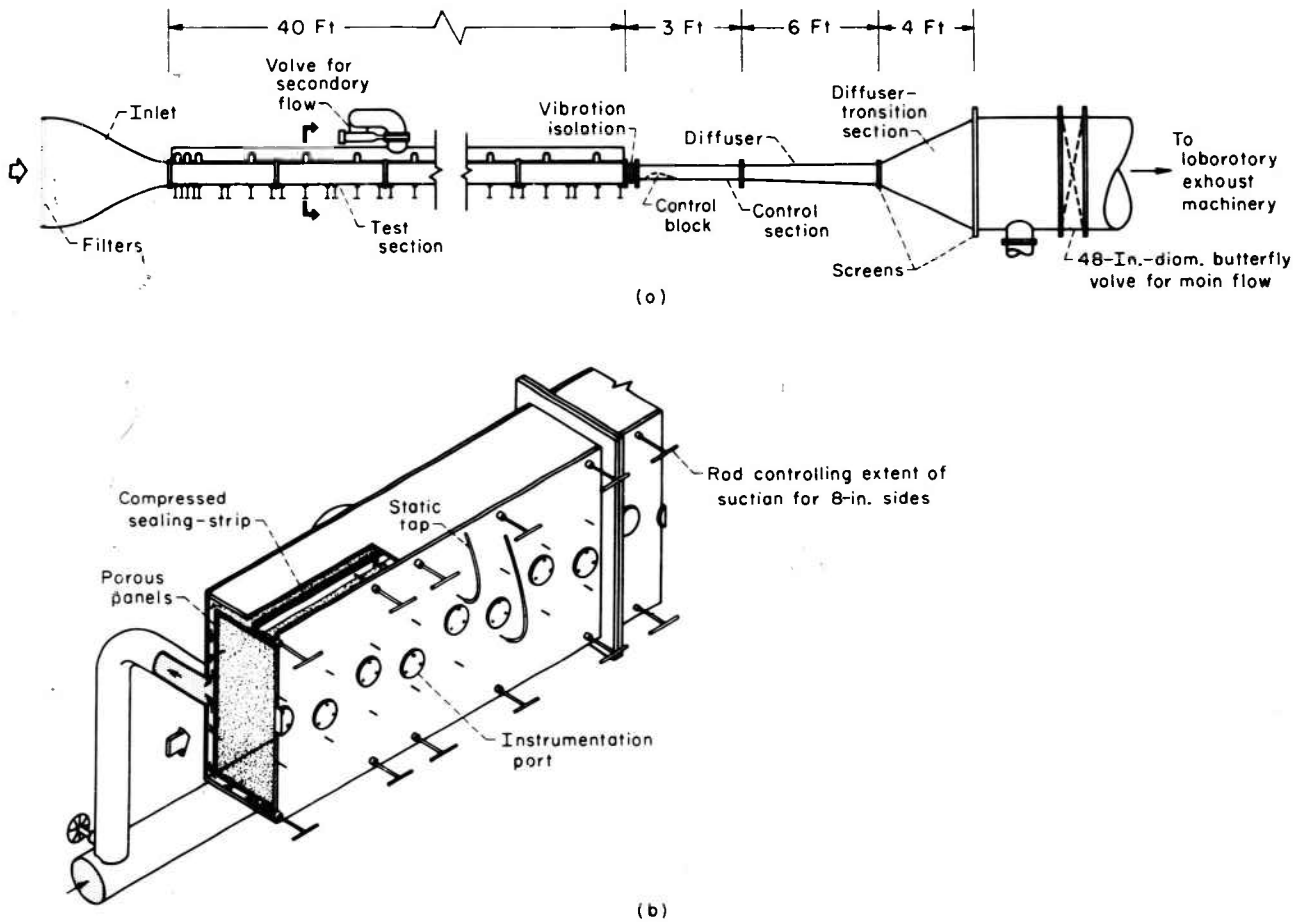

Fig.1 Wind-tunnel facility: (a) complete wind tunnel, (b) test-section detail

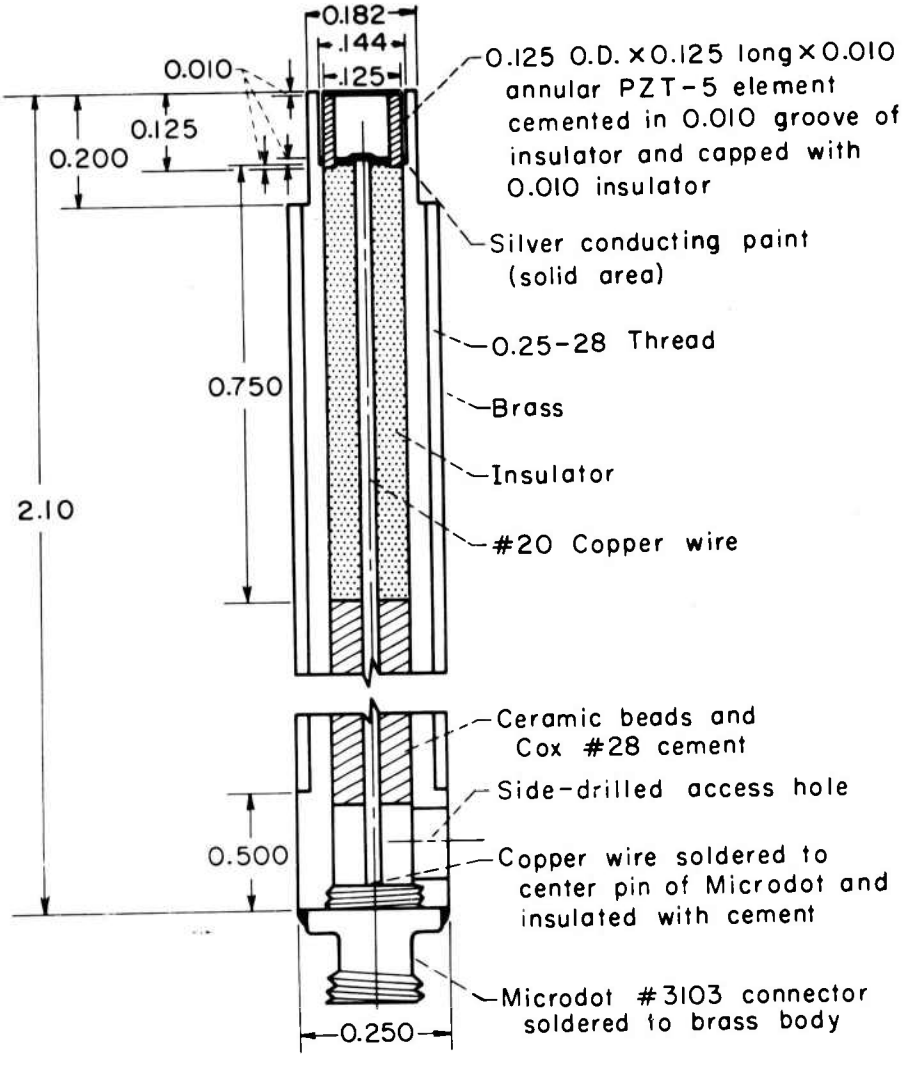

(Dimensions are in inches.)

Fig.2 Piezoelectric transducer for measuring fluctuating pressures

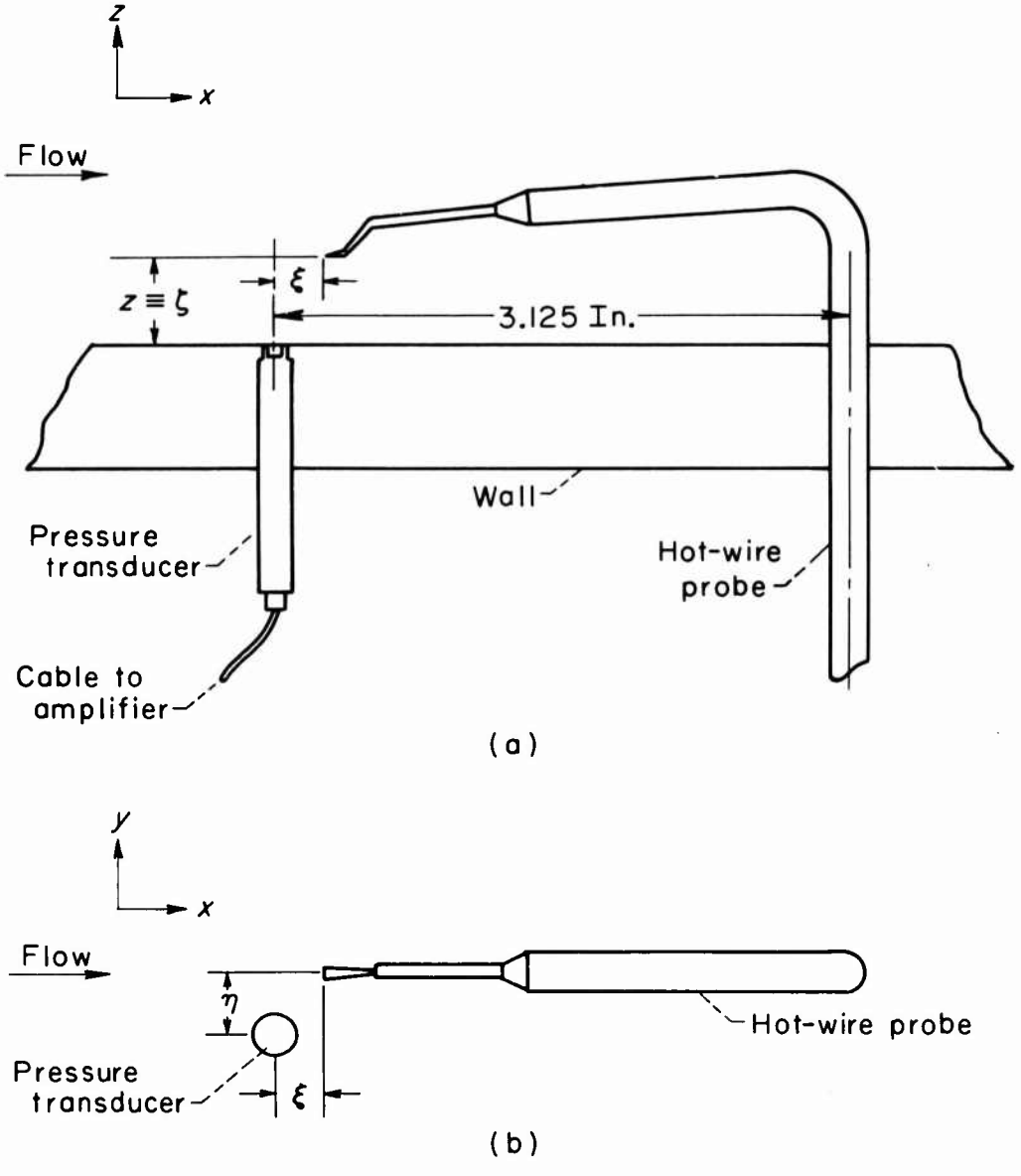

Fig.3 Spatial relation of hot-wire and pressure transducer: (a) side view, (b) plan view

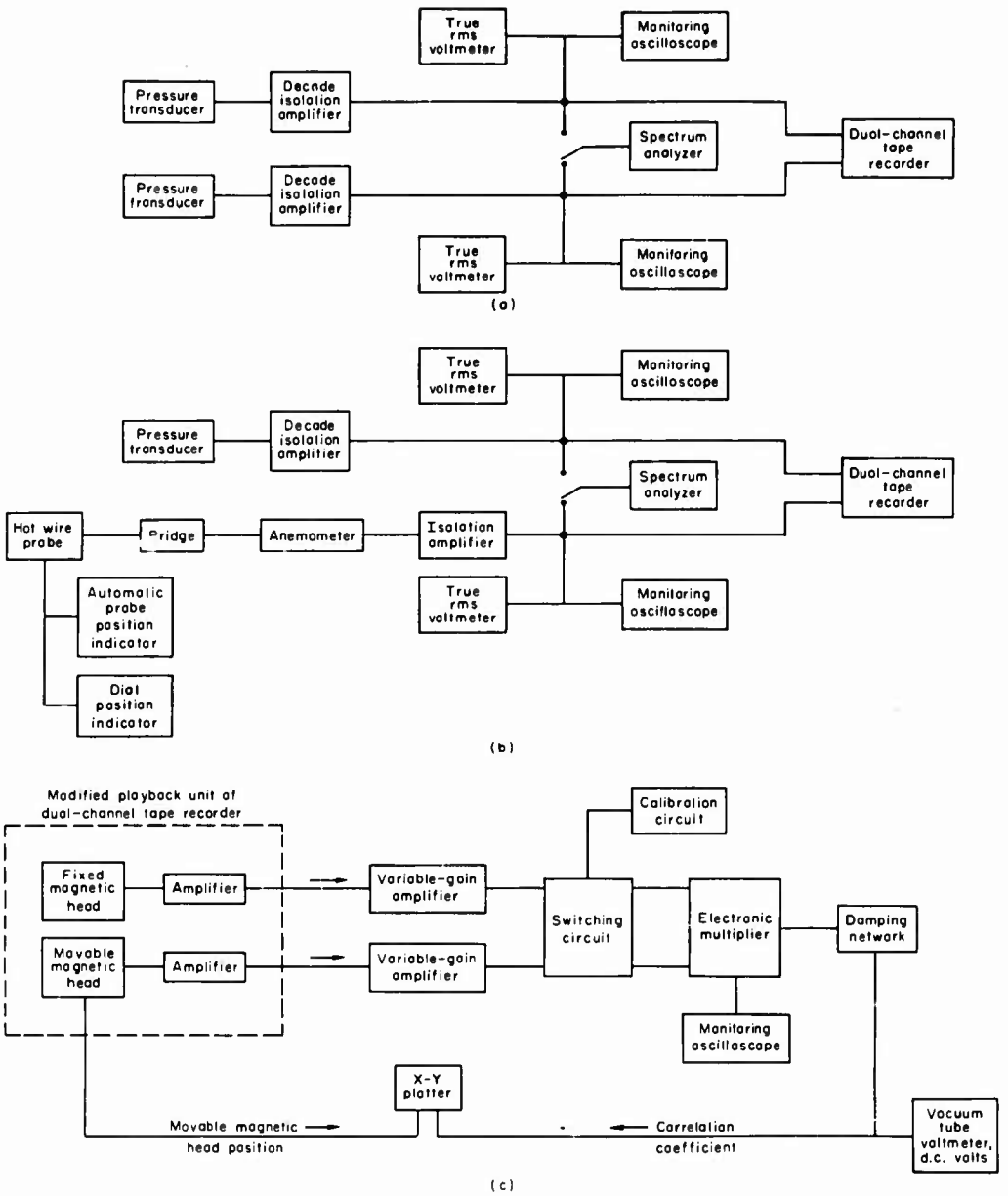

Fig. 4 Block diagrams of instrumentation in taking data for (a) correlations of wall-pressure fluctuations, (b) correlations of velocity fluctuations with wall-pressure fluctuations. Correlation computer (diagram C)

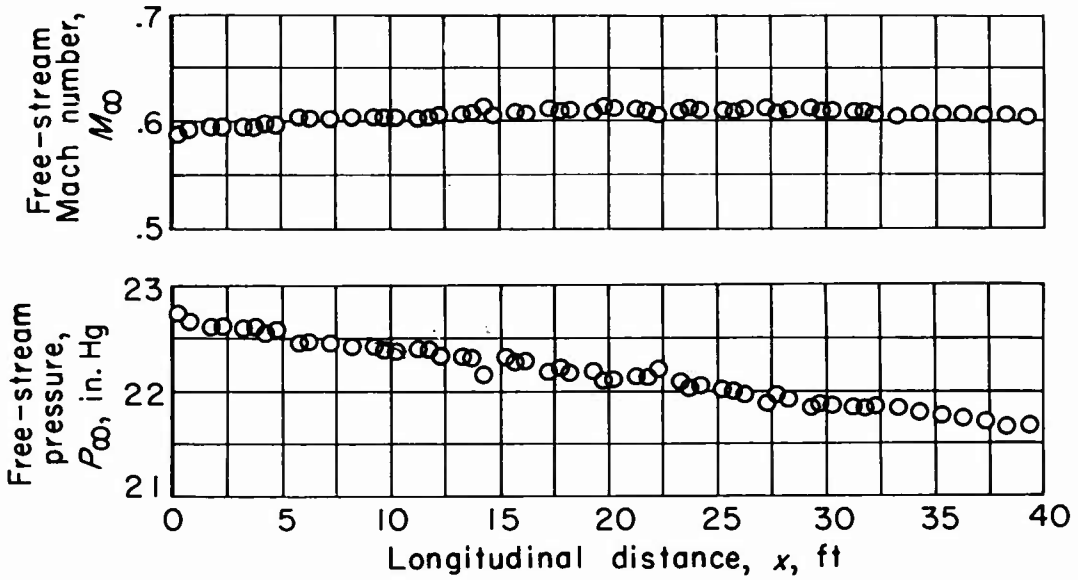

Fig. 5 Longitudinal variation of free-stream pressure and Mach number at centerline of wind tunnel

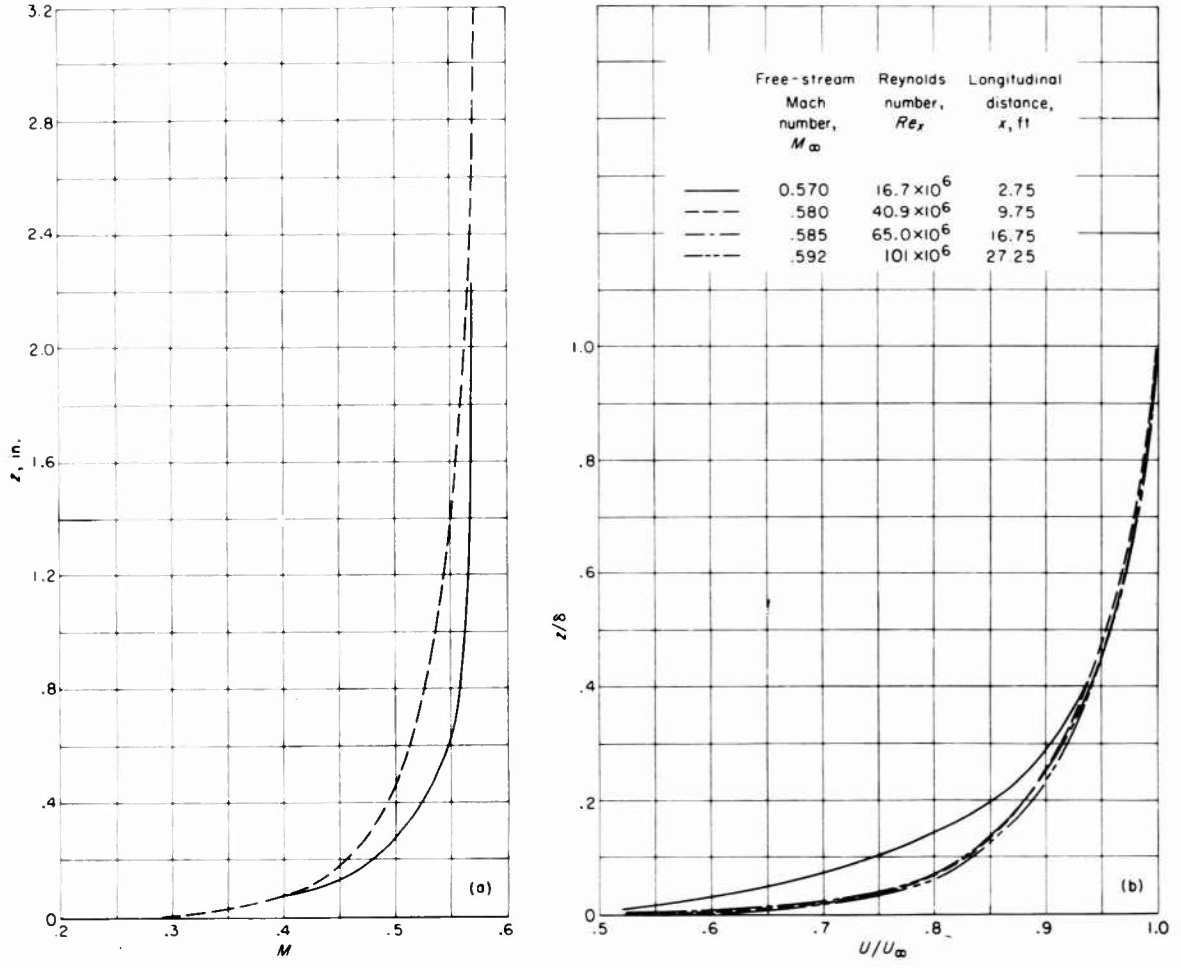

Fig.6 Typical boundary-layer mean velocity profiles: (a) Mach number as a function of distance from wall, (b) dimensionless velocity as a function of dimensionless distance from wall

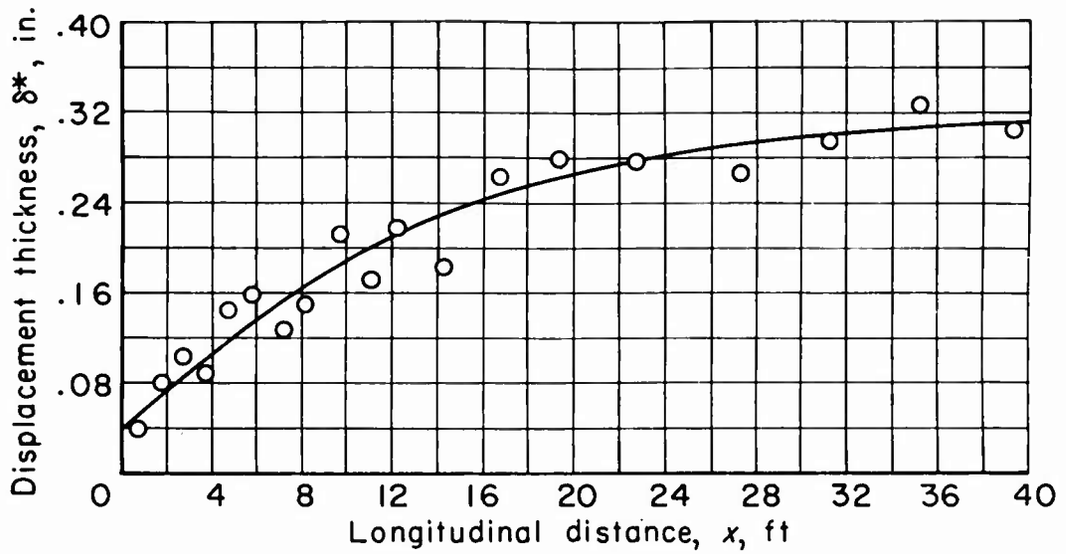

Fig. 7 Variation of displacement thickness with longitudinal distance. Free-stream Mach number, 0.60; Reynolds number per foot, 3.56×10^6

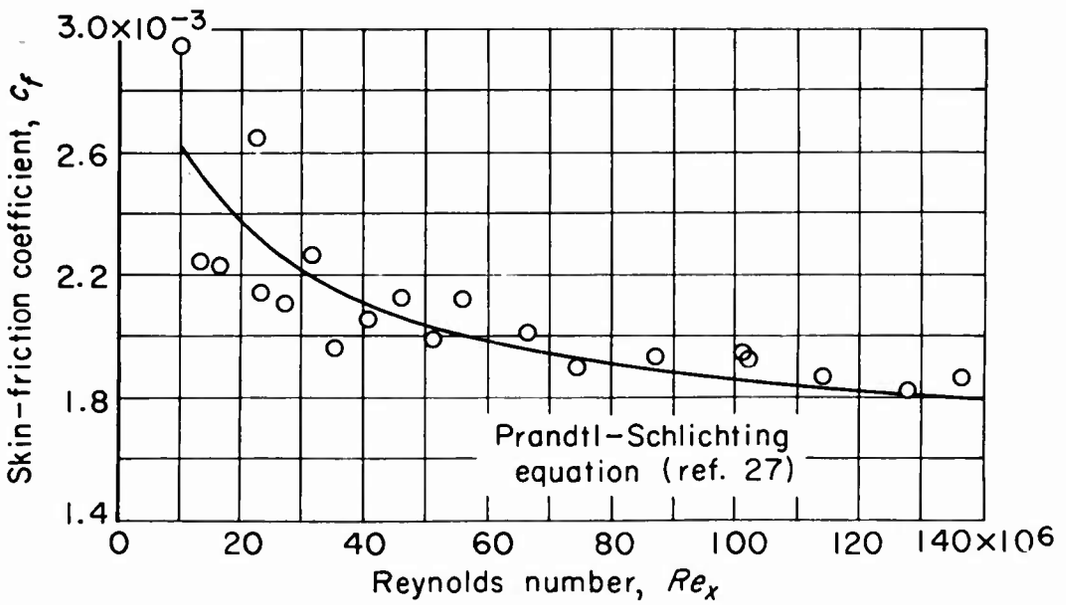

Fig. 8 Local skin-friction coefficients as a function of Reynolds number

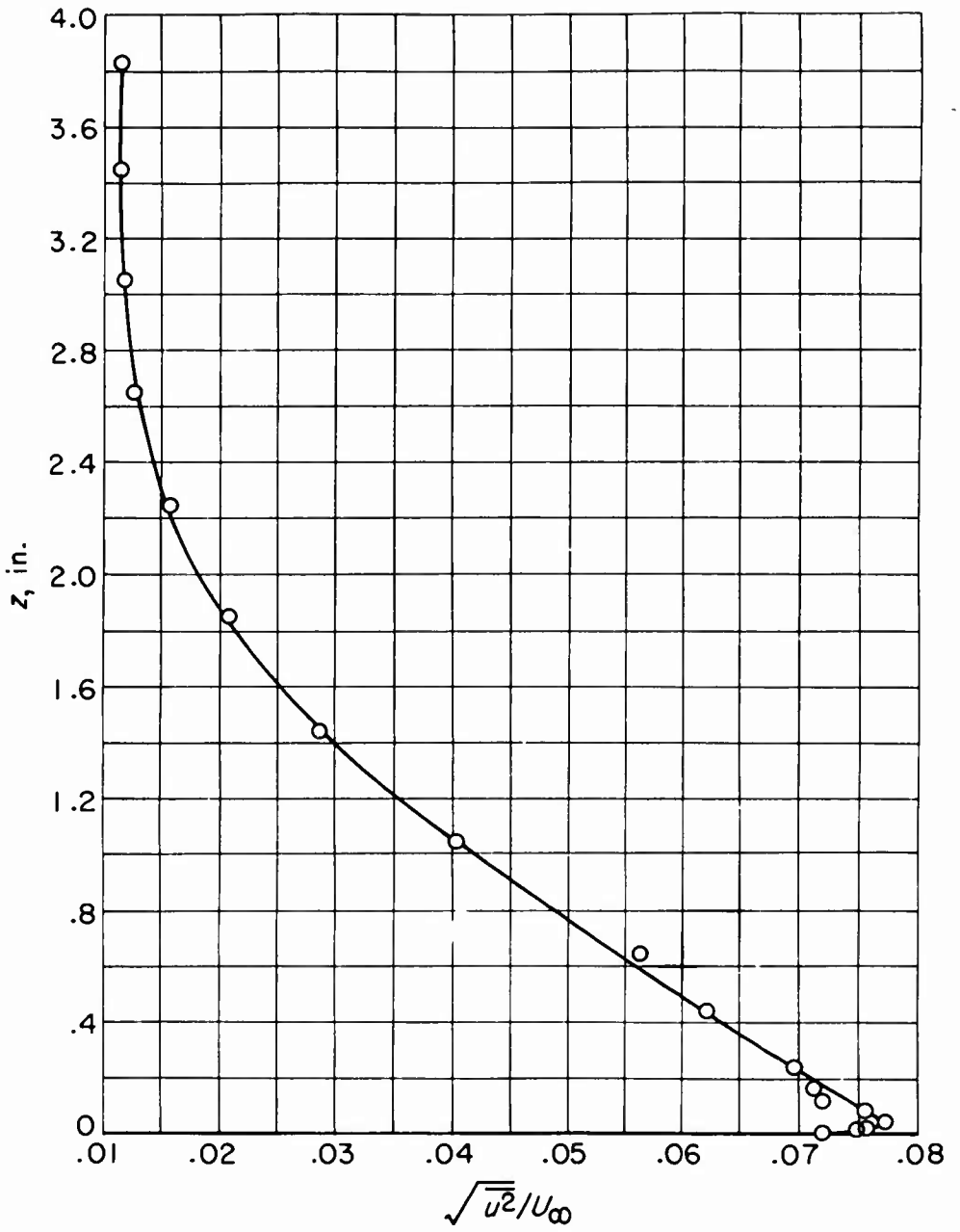

Fig.9 Boundary-layer profile of ratio of longitudinal intensity to free-stream velocity. Longitudinal distance, 9.25 feet; free-stream Mach number, 0.605; Reynolds number, 3.98×10^7

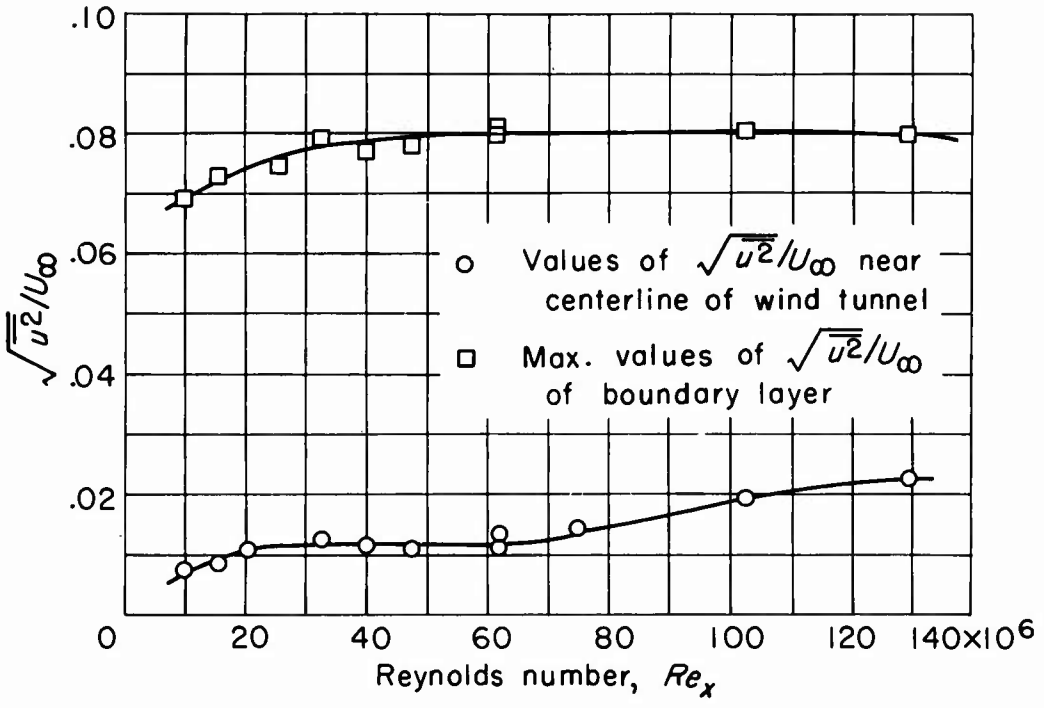

Fig.10 Variation of turbulent intensity with Reynolds number based on effective turbulent length $(x - x_0)$

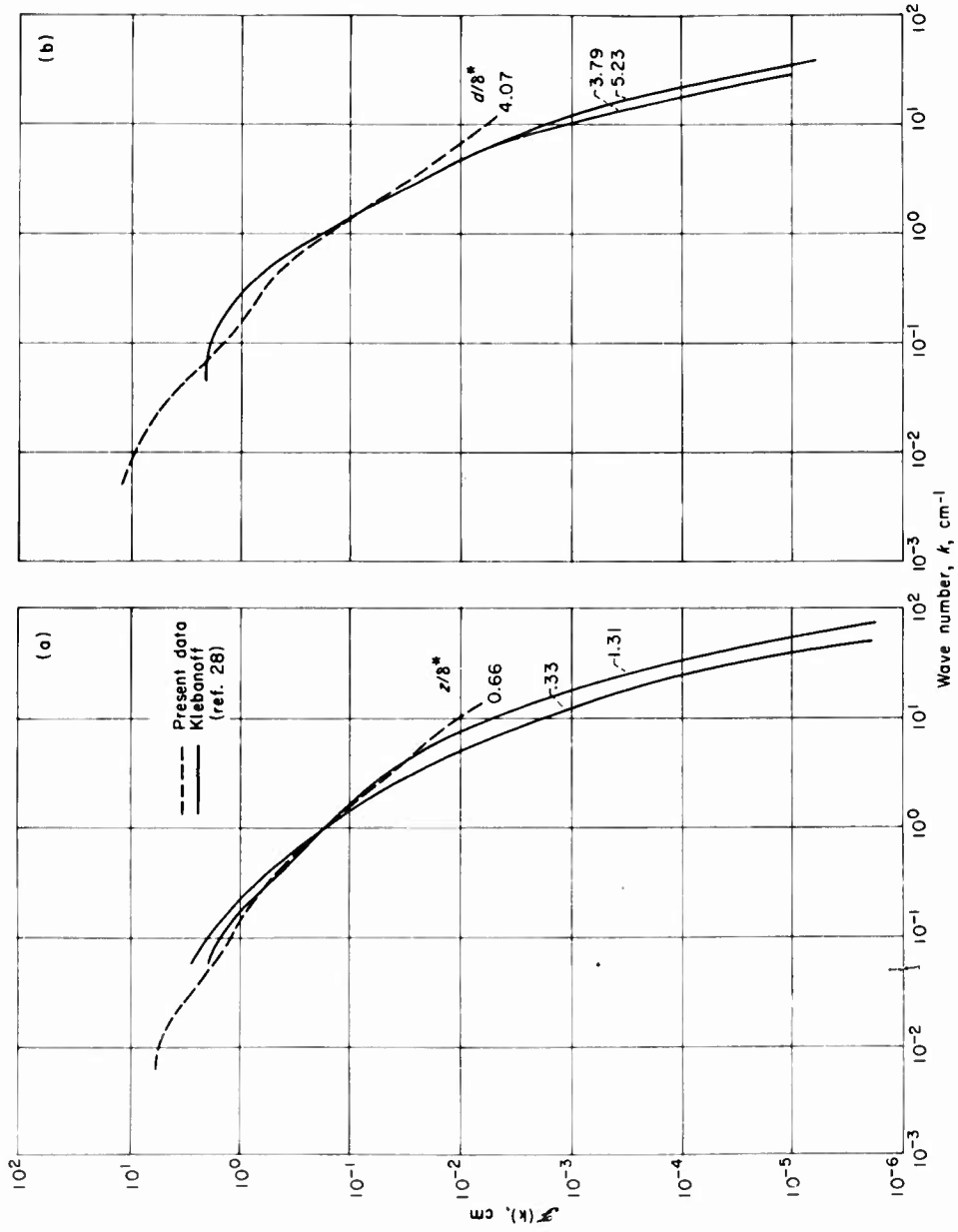

Fig.11 Comparison of u-fluctuation spectra with Klebanoff's data[28] (a) inner region of boundary layer, (b) outer region of boundary layer

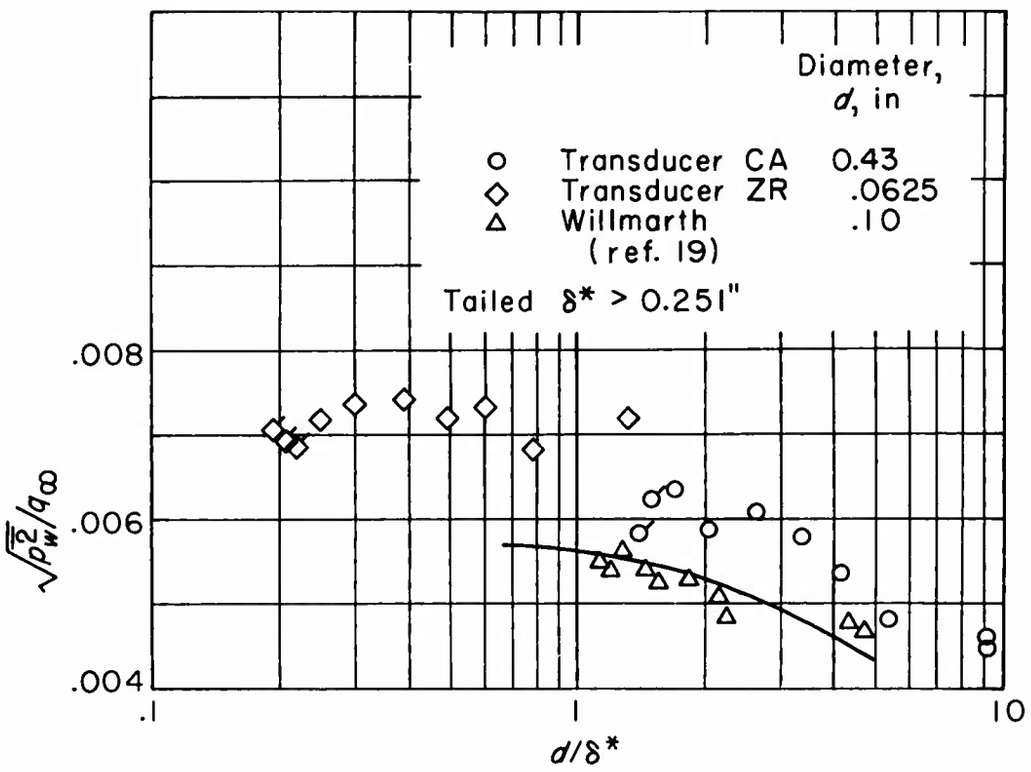

Fig. 12 Comparison of root-mean-square wall-pressure fluctuations with Willmarth's data[19]

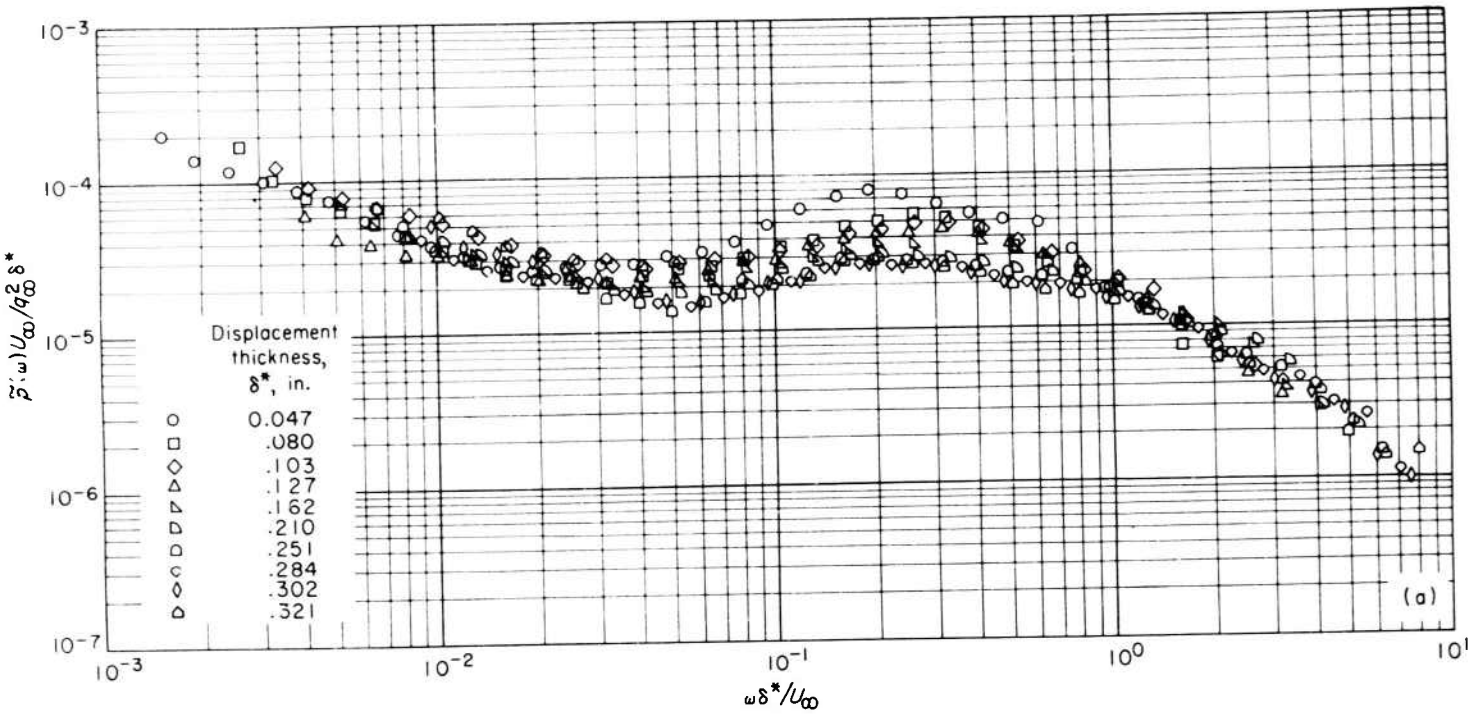

Fig. 13(a) Transducer ZR ; diameter, 0.0625 inch. Mean-square spectra of wall-pressure fluctuations. Free-stream Mach number, 0.60; Reynolds number per foot, 3.45×10^6

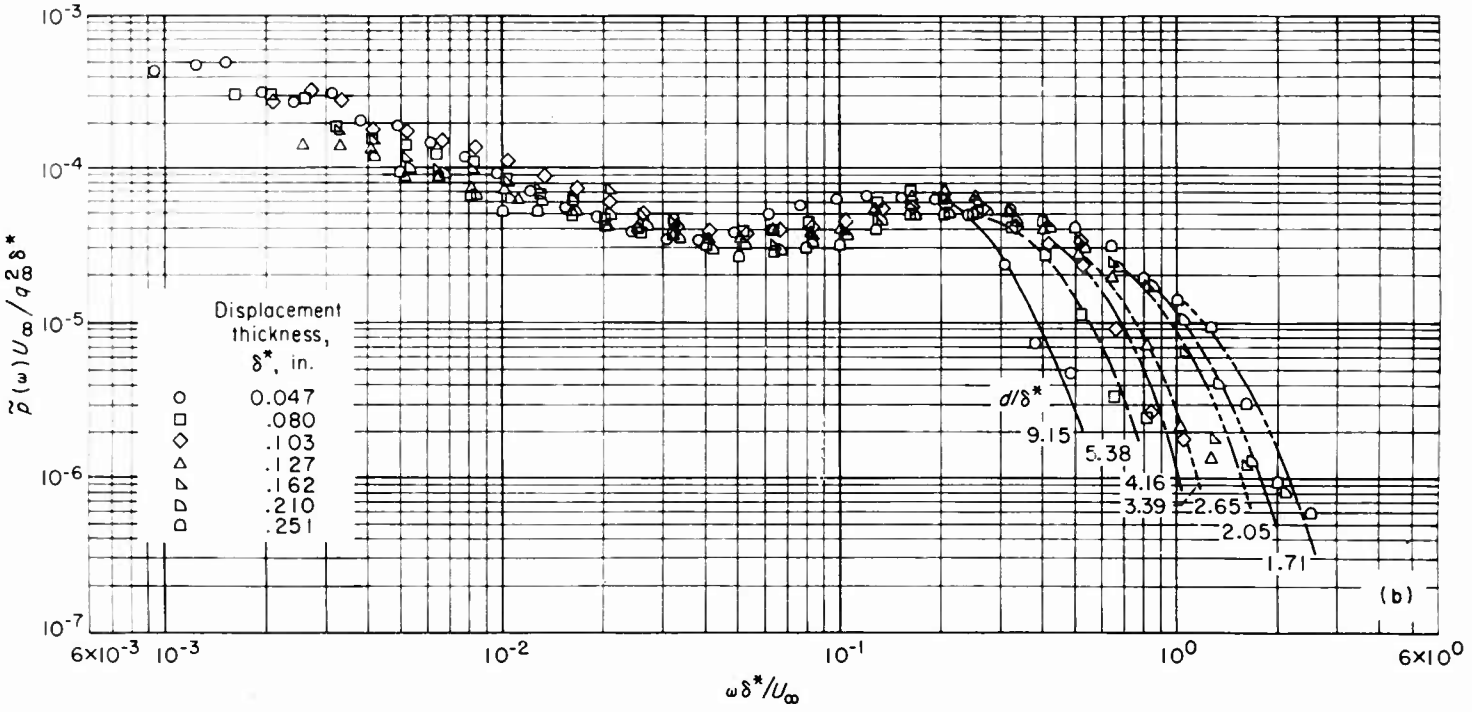

Fig. 13(b) Transducer CA ; diameter, 0.43 inch. Mean-square spectra of wall-pressure fluctuations. Free-stream Mach number, 0.60; Reynolds number per foot, 3.45×10^6

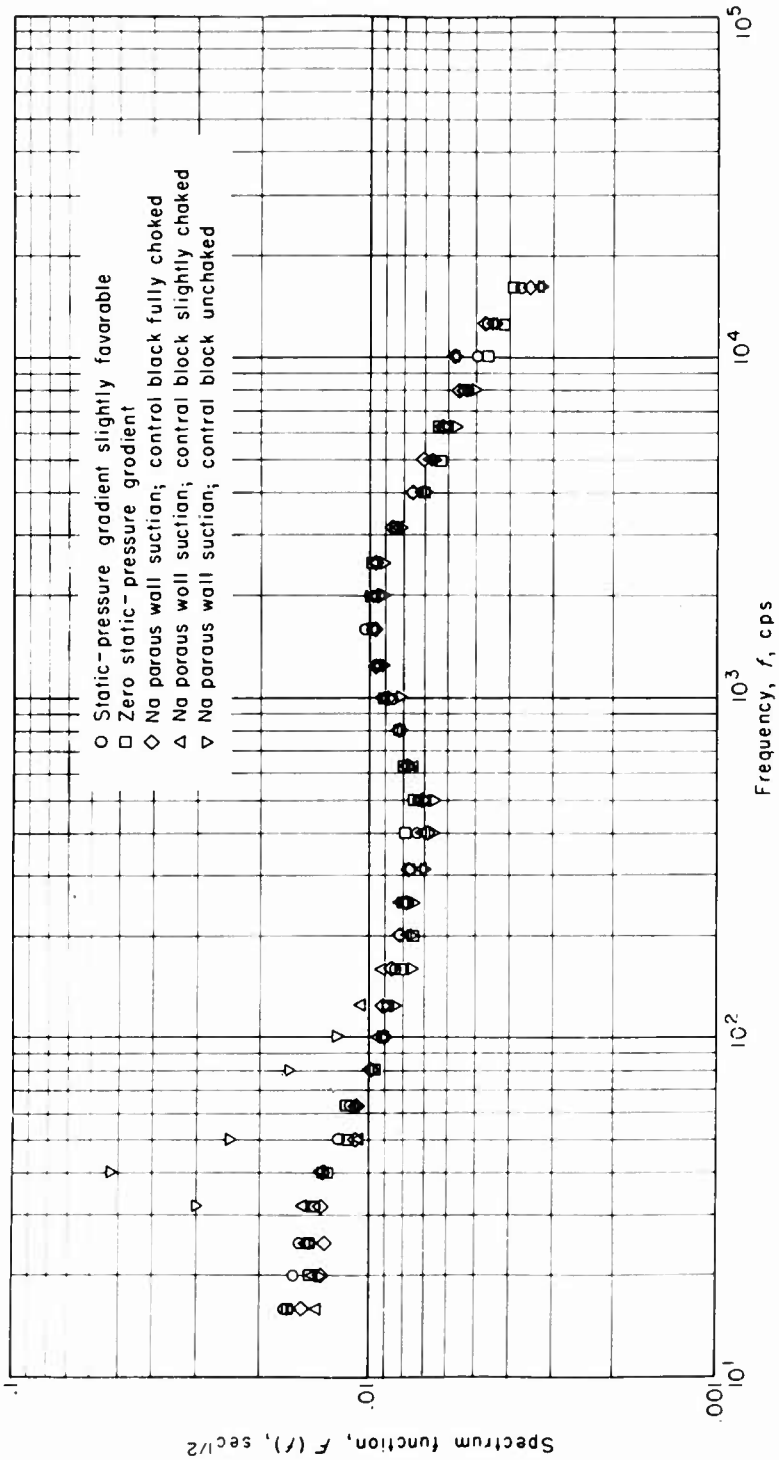

Fig.14 Comparison of spectra of wall-pressure fluctuations for various flow conditions in test section. Transducer CB ; diameter, 0.040 inch; free-stream Mach number, 0.60; Reynolds number per foot, 3.45×10^6

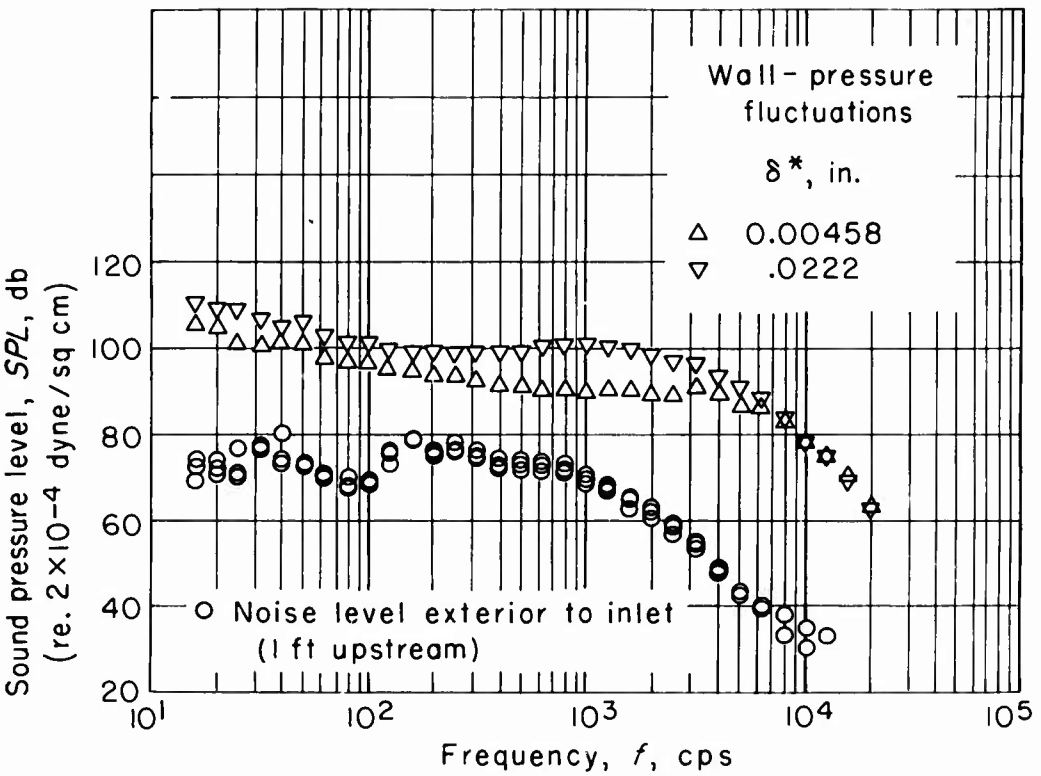

Fig.15 Comparison of spectra of noise levels measured at inlet of wind tunnel with spectra of wall-pressure fluctuations. Transducer CA ; diameter, 0.43 inch. (For external noise measurements microphone faced upward and downstream)

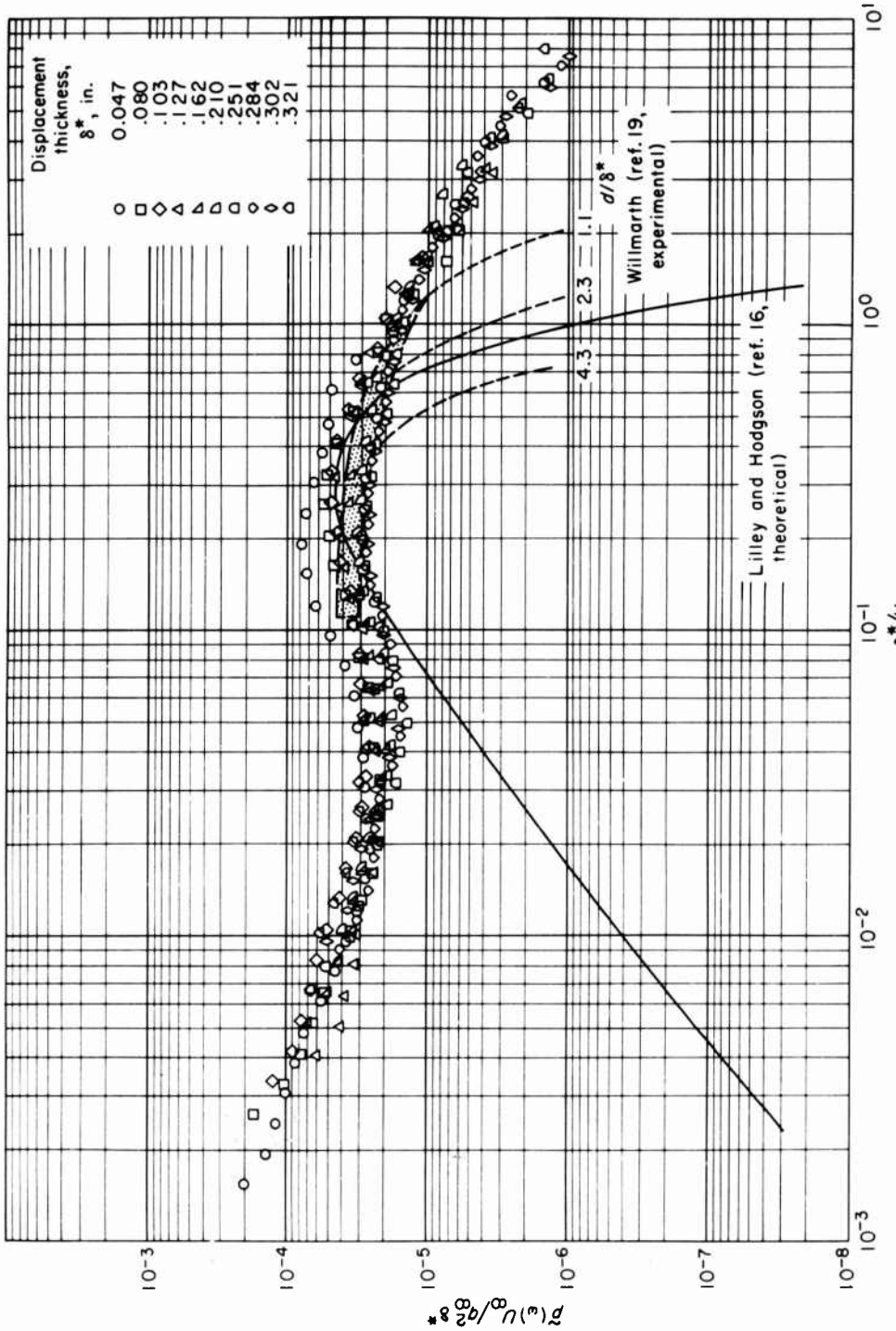

Fig. 16 Comparison of dimensionless mean-square spectra with results of other investigations. Free-stream Mach number, 0.60; Reynolds number per foot, 3.45×10^6

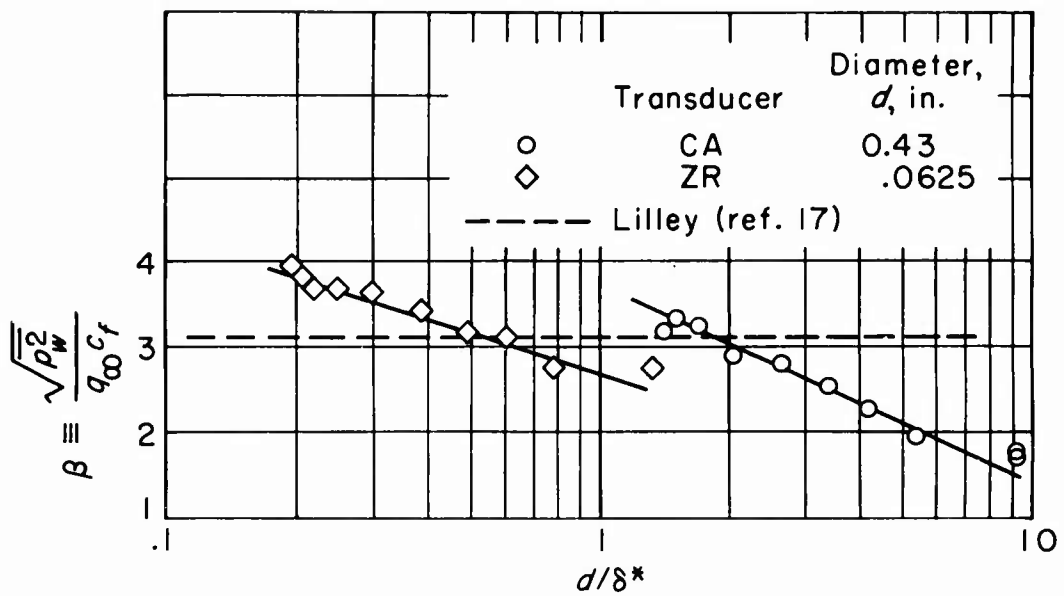

Fig. 17 Comparison of experimental values of root-mean-square magnitude of wall-pressure fluctuations with Lilley's theory[17]

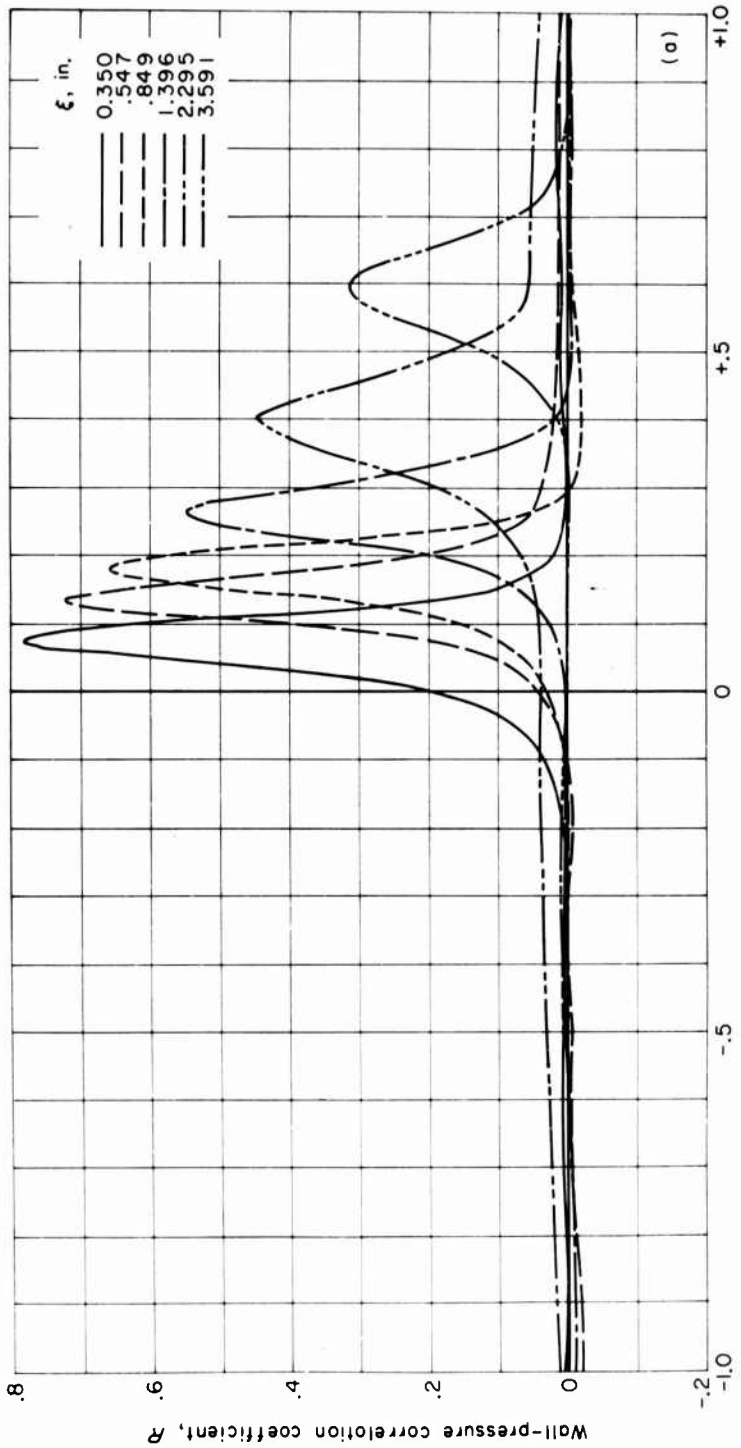

Fig. 18(a) Correlation of wall-pressure fluctuations at two points as a function of time delay; $\xi = 0.88$ inch and $\eta = 0$

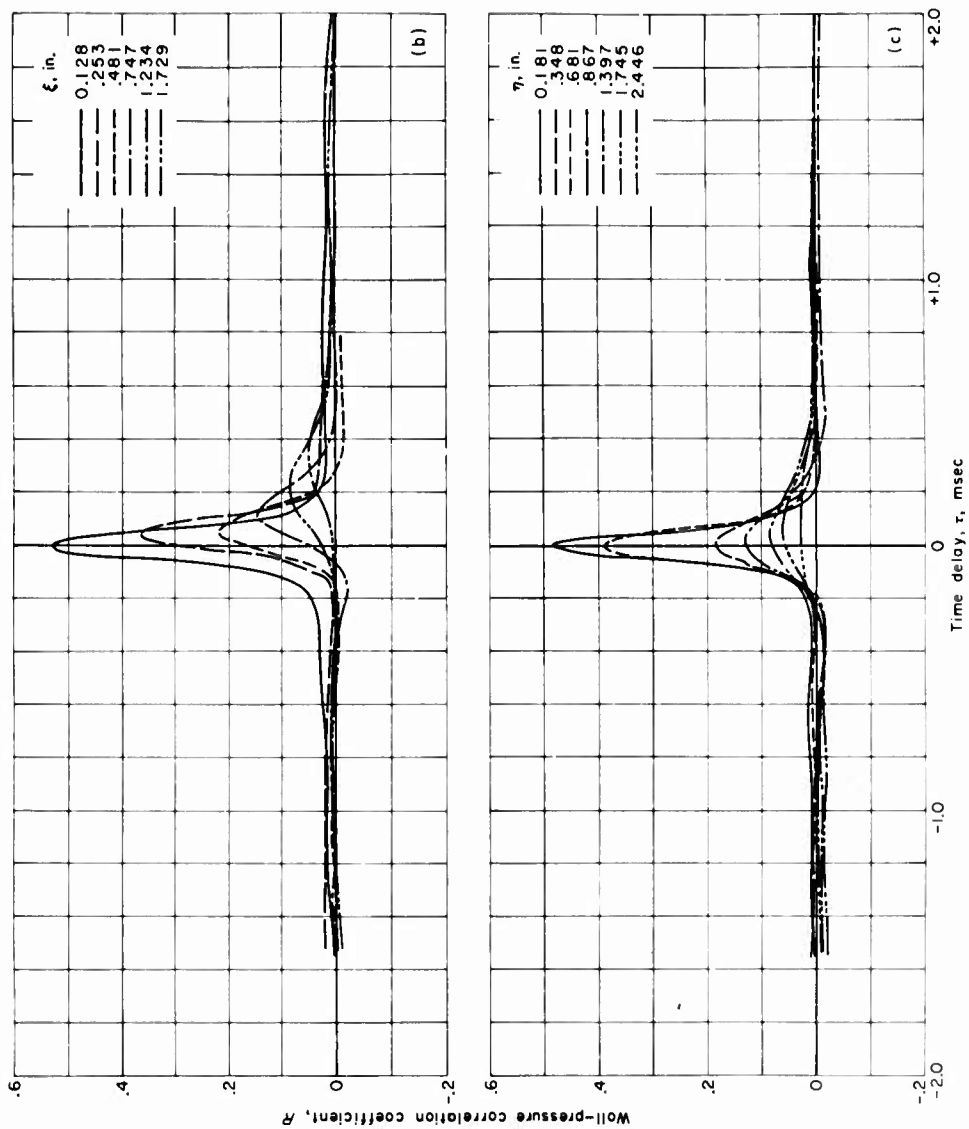

Fig. 18 Correlation of wall-pressure fluctuations at two points as a function of time delay: (b) $\eta = \xi$; (c) $\xi = 0$

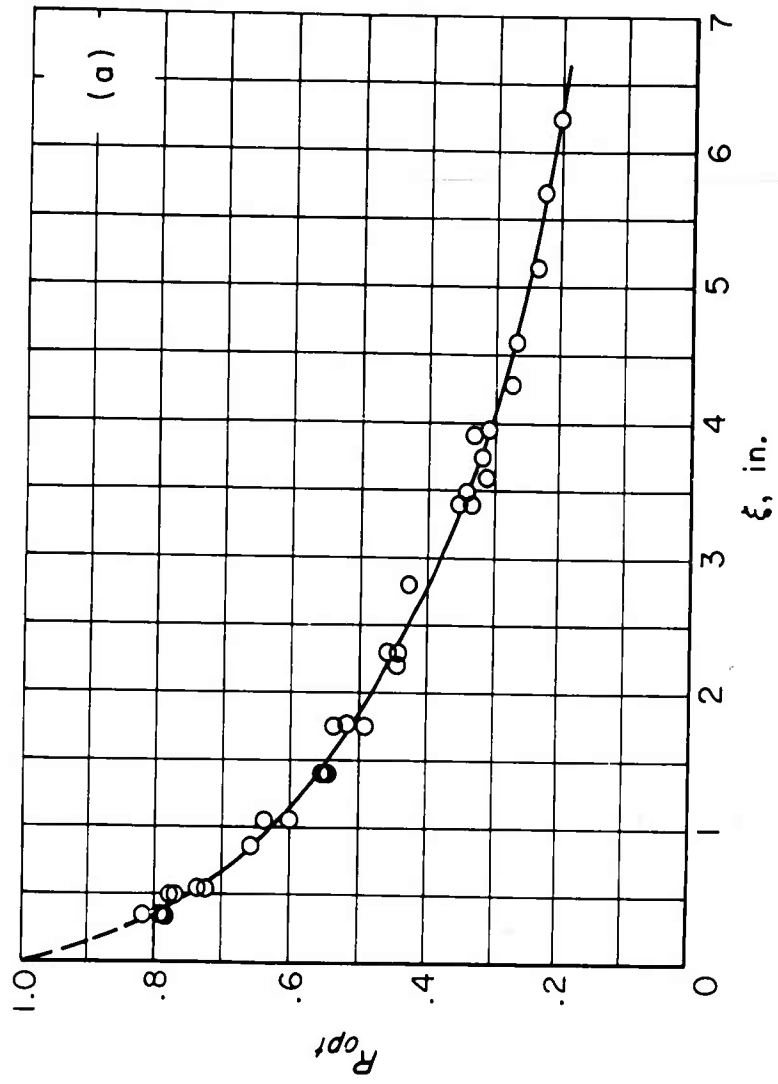

Fig. 19(a) Optimum correlation of wall-pressure fluctuations as a function of ξ; $\eta = 0$

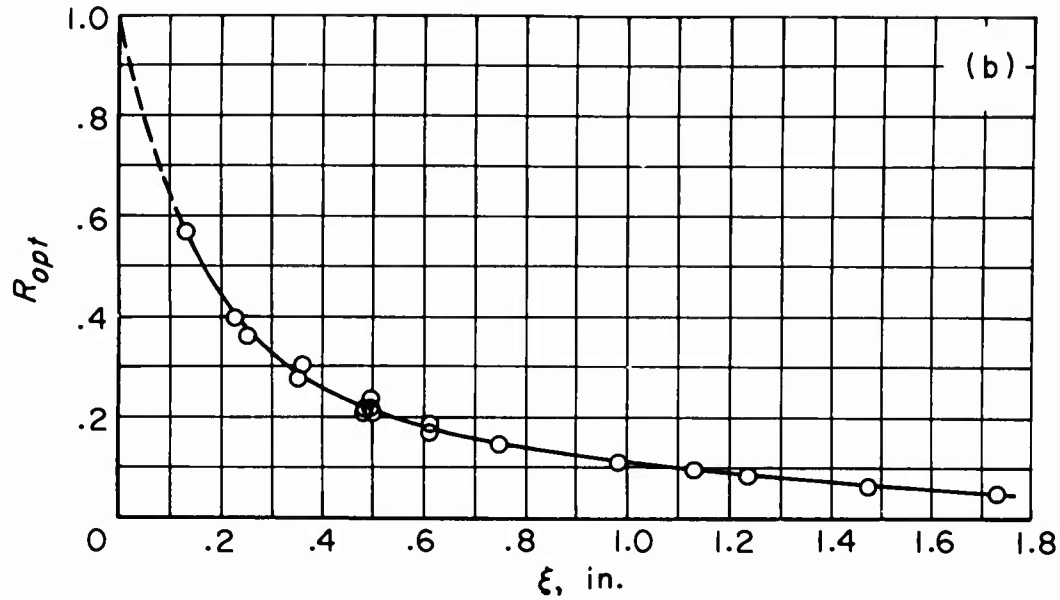

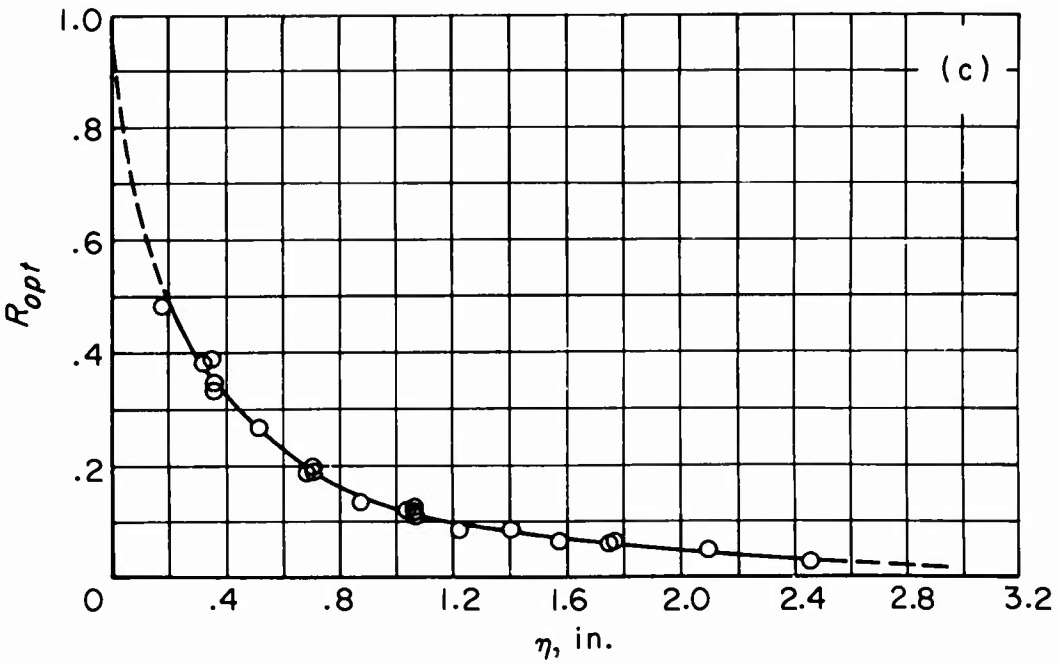

Fig. 19 (b) & (c) Optimum correlation of wall-pressure fluctuations: (b) as a function of ξ ; $\xi = \eta$; (c) as a function of η ; $\xi = 0$

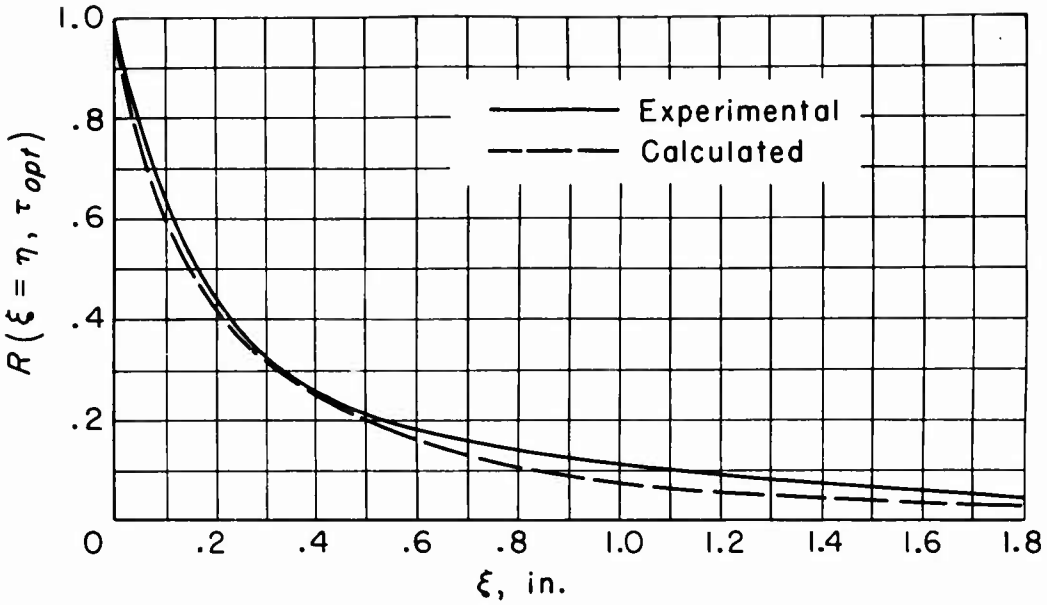

Fig. 20 Comparison for $R_{opt}(\xi = \eta, \tau_{opt})$ of experimental curve with that calculated from optimum correlations obtained for $\xi = 0$ and $\eta = 0$

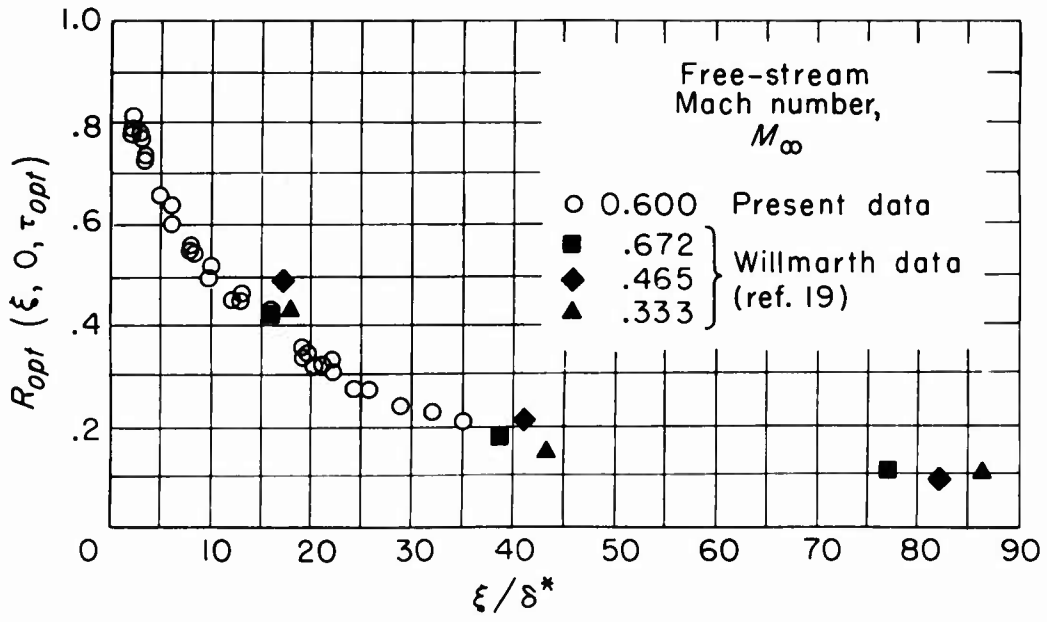

Fig. 21 Comparison of correlation coefficient $R_{opt}(\xi, 0, \tau_{opt})$ with Willmarth's data[19]. $\eta = 0$

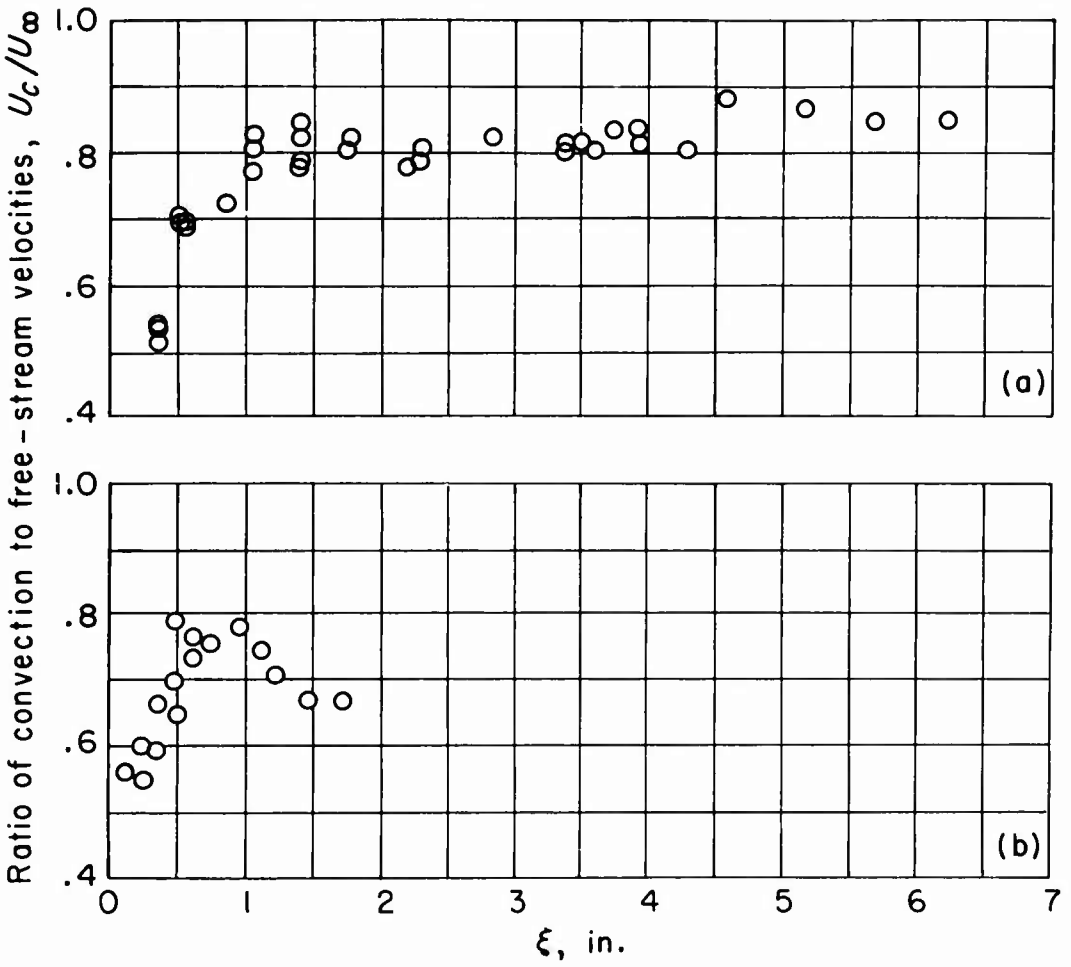

Fig. 22 Ratio of convection to free-stream velocities as a function of ξ-component of separation distance for (a) $\eta = 0$; (b) $\xi = \eta$

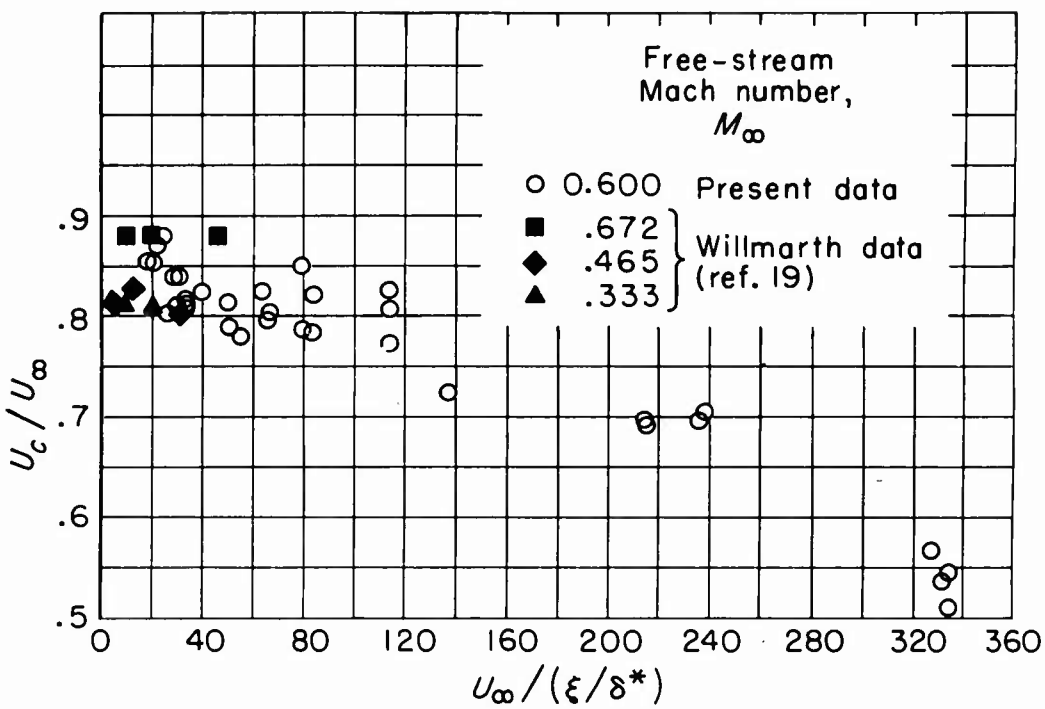

Fig. 23 Comparison of ratio of convection to free-stream velocities with Willmarth's data[19]. $\eta = 0$

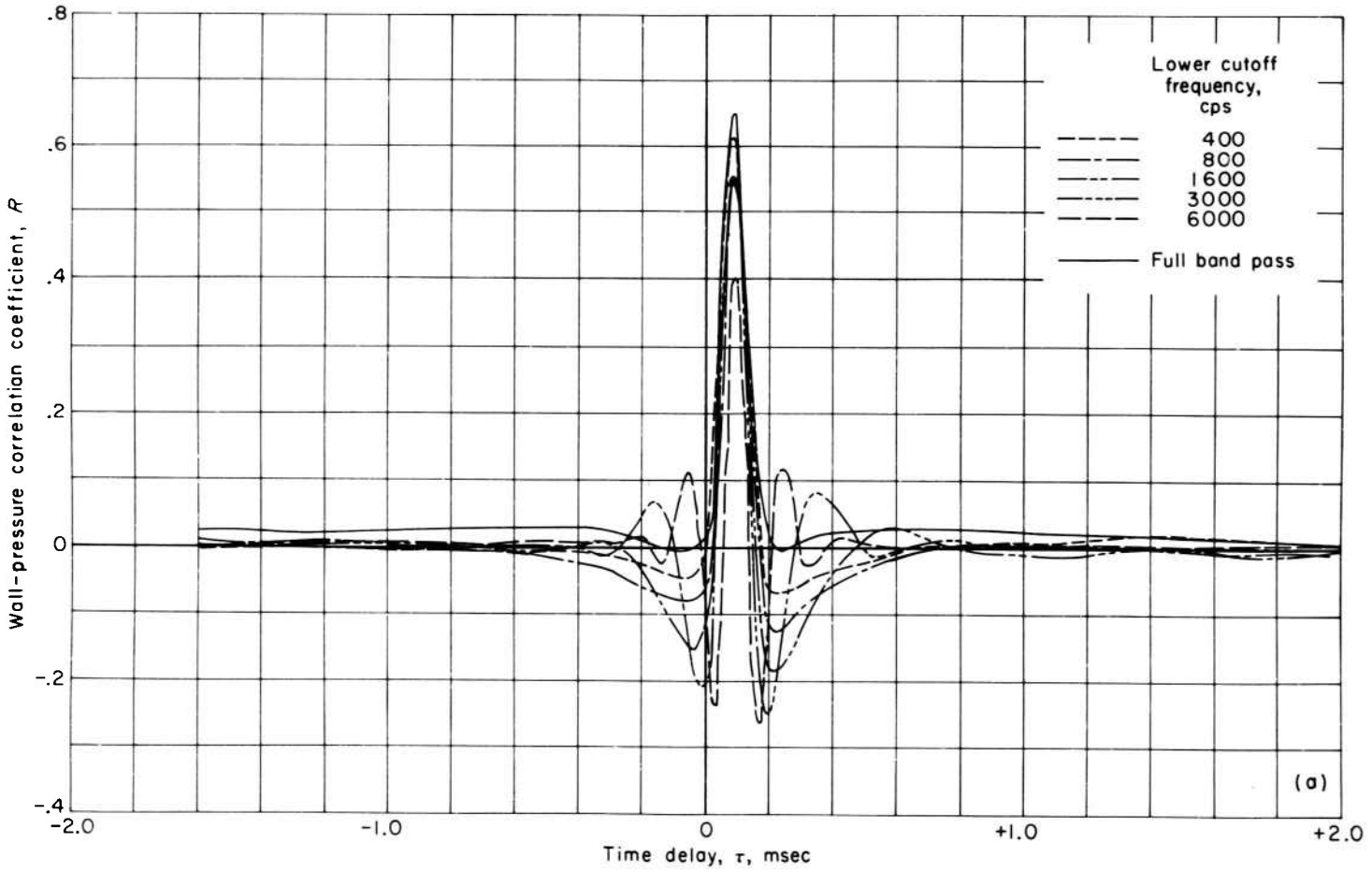

Fig. 24(a) Effect of high-pass-band filtering on correlation of wall-pressure fluctuations as a function of time delay for $\xi = 0.88$ inch and $\eta = 0$

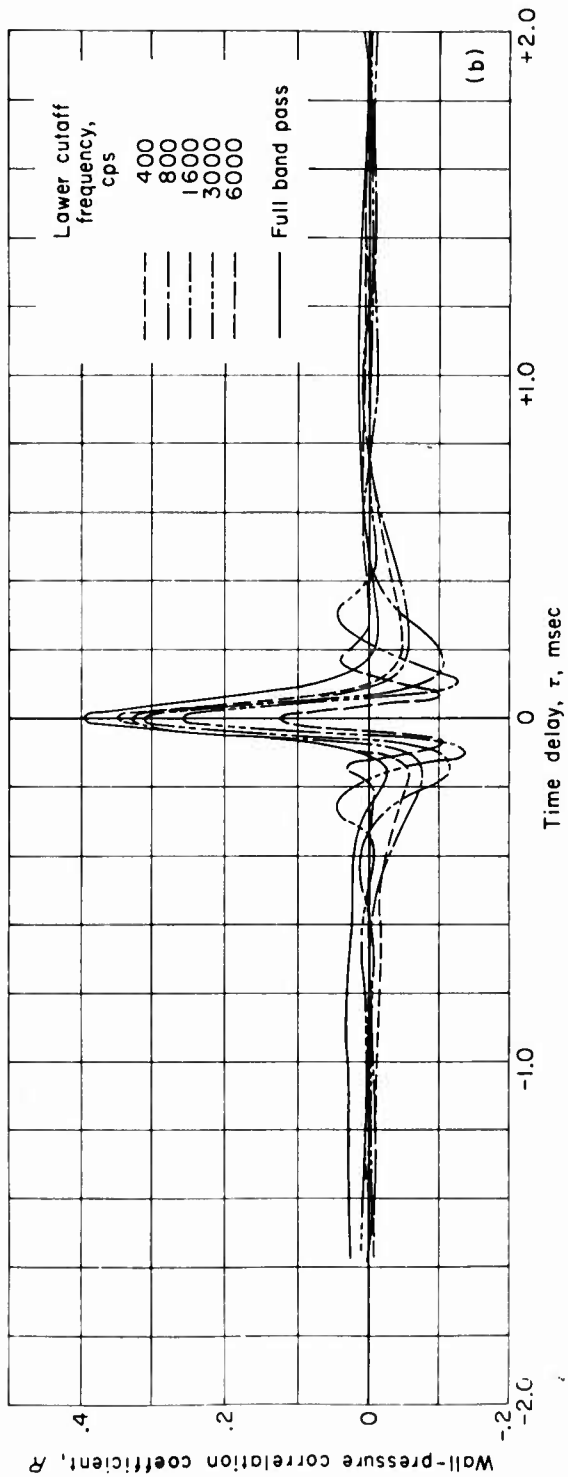

Fig.24(b) Effect of high-pass-band filtering on correlation of wall-pressure fluctuations as a function of time delay for $\xi = 0$ and $\eta = 0.325$ inch

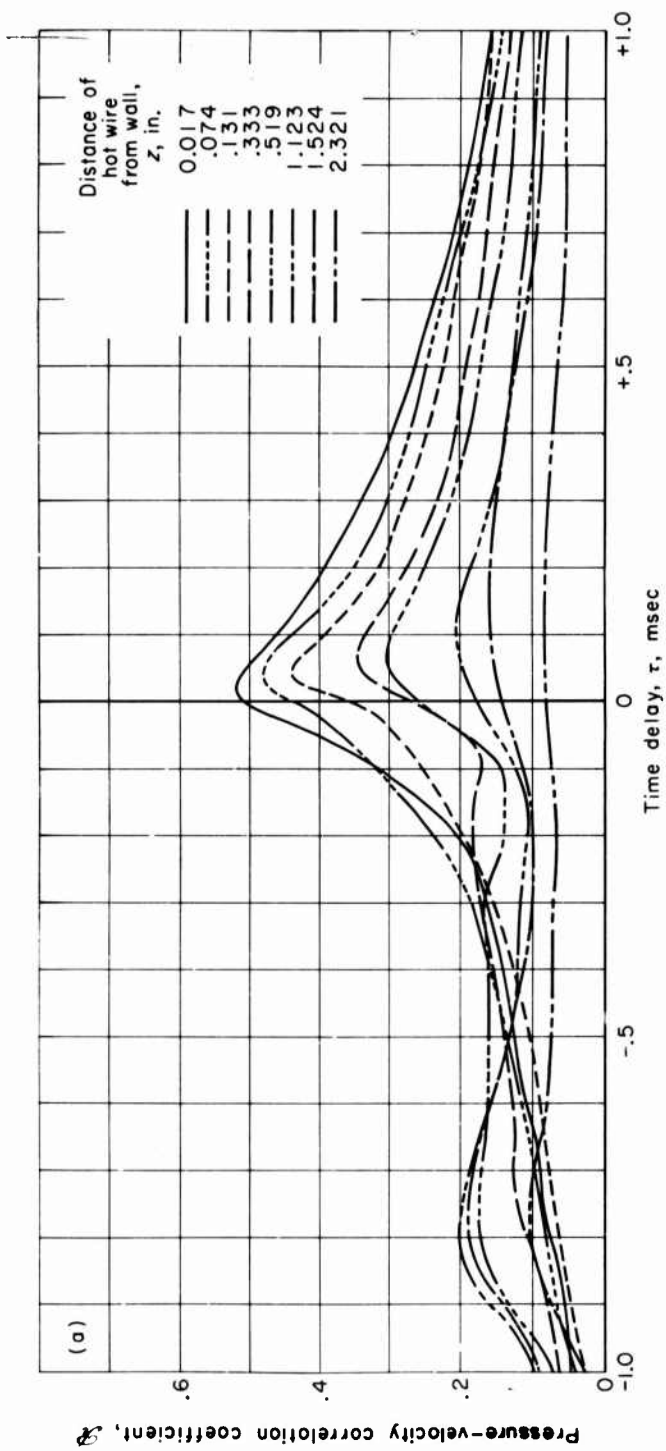

Fig. 25(a) Correlation of velocity fluctuations with wall-pressure fluctuations, measured with transducer ZS . $\eta \approx 0$ and $\xi = -0.001$ inch

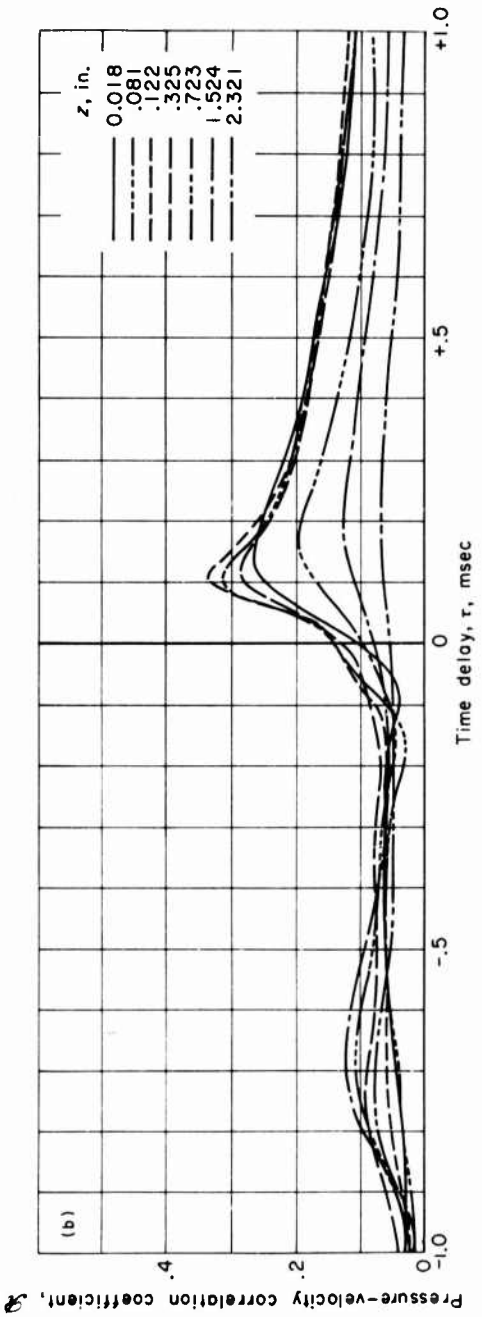

Fig. 25(b) Correlation of velocity fluctuations with wall-pressure fluctuations, measured with transducer ZS . $\eta \approx 0$ and $\xi = 0.307$ inch

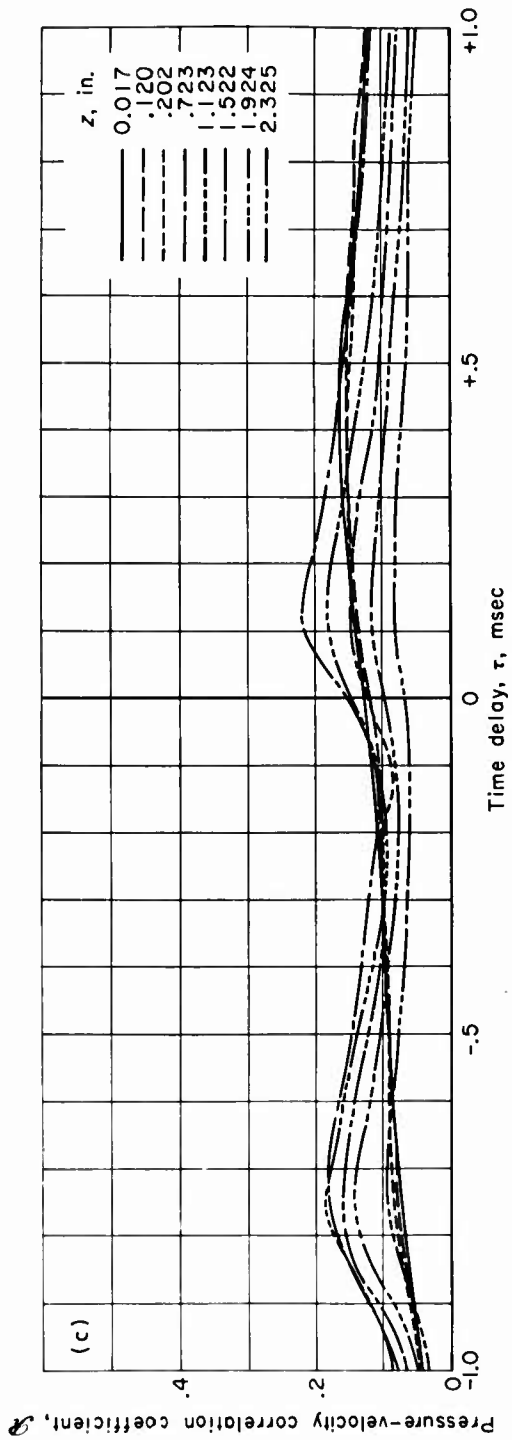

Fig. 25(c) Correlation of velocity fluctuations with wall-pressure fluctuations, measured with transducer ZS . $\xi \approx 0$ and $\eta = 0.390$ inch

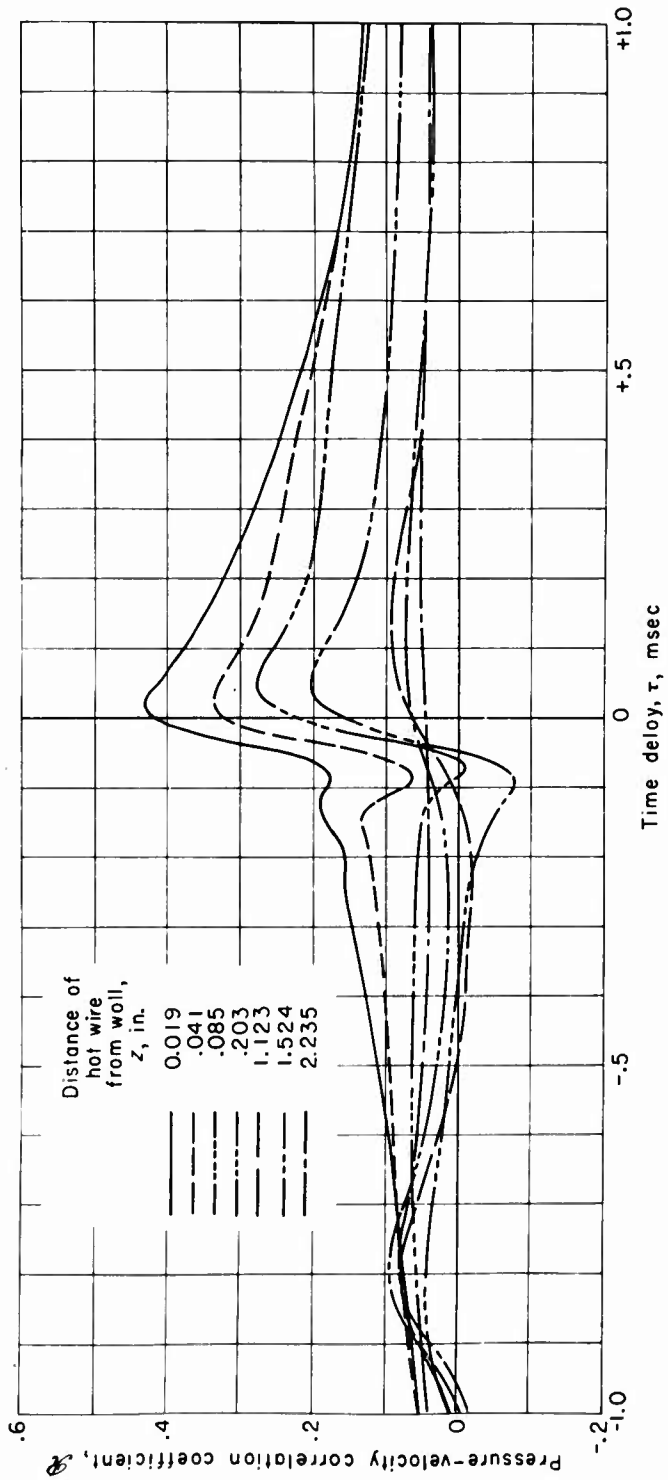

Fig.26 Correlation of velocity fluctuations with wall-pressure fluctuations, measured with transducer CB . $\xi \approx 0$; $\eta = 0.003$ inch

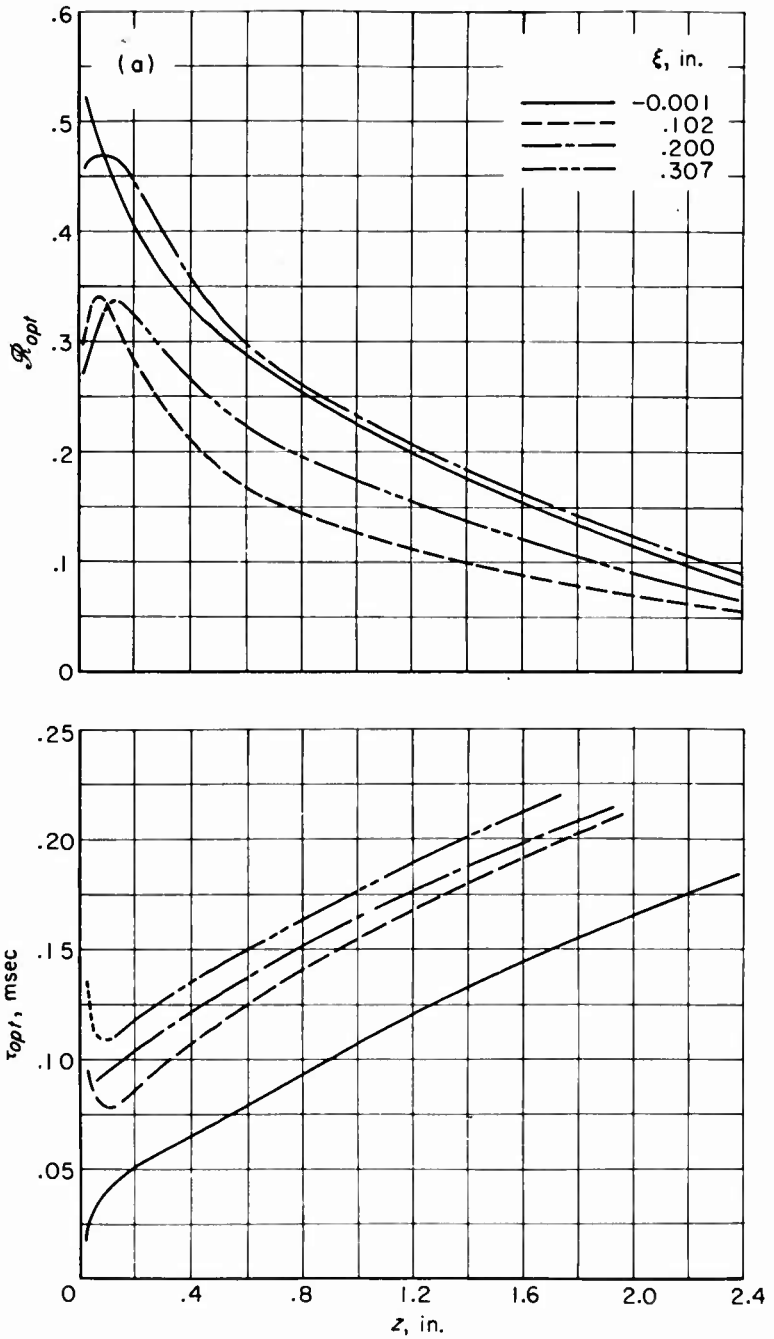

Fig. 27(a) Significant characteristics obtained from correlation of velocity fluctuations with wall-pressure fluctuations, transducer ZS . $\eta \approx 0$
(See also next page)

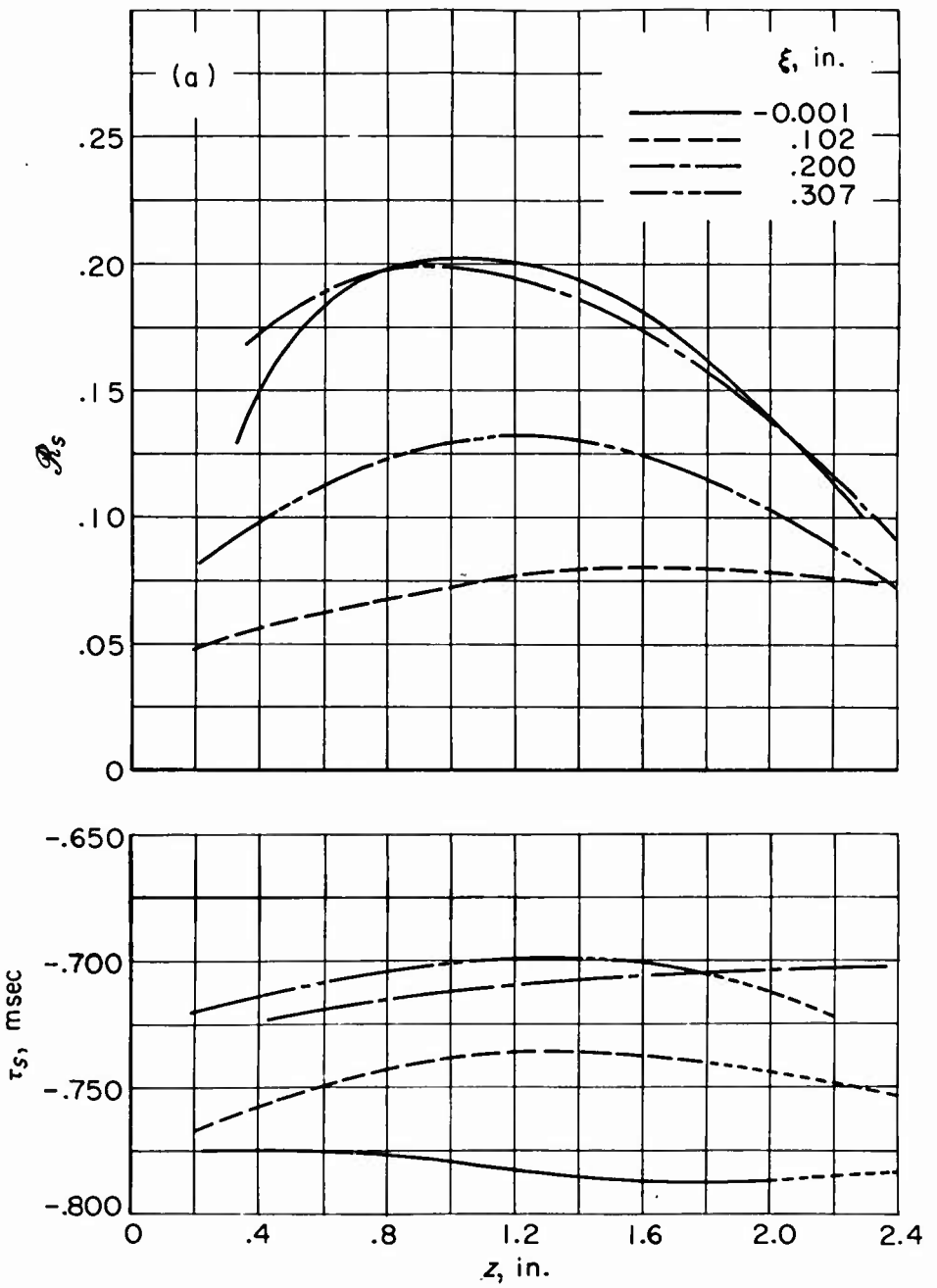

Fig. 27(a) (continued) Significant characteristics obtained from correlation of velocity fluctuations with wall-pressure fluctuations, transducer ZS . $\eta \approx 0$

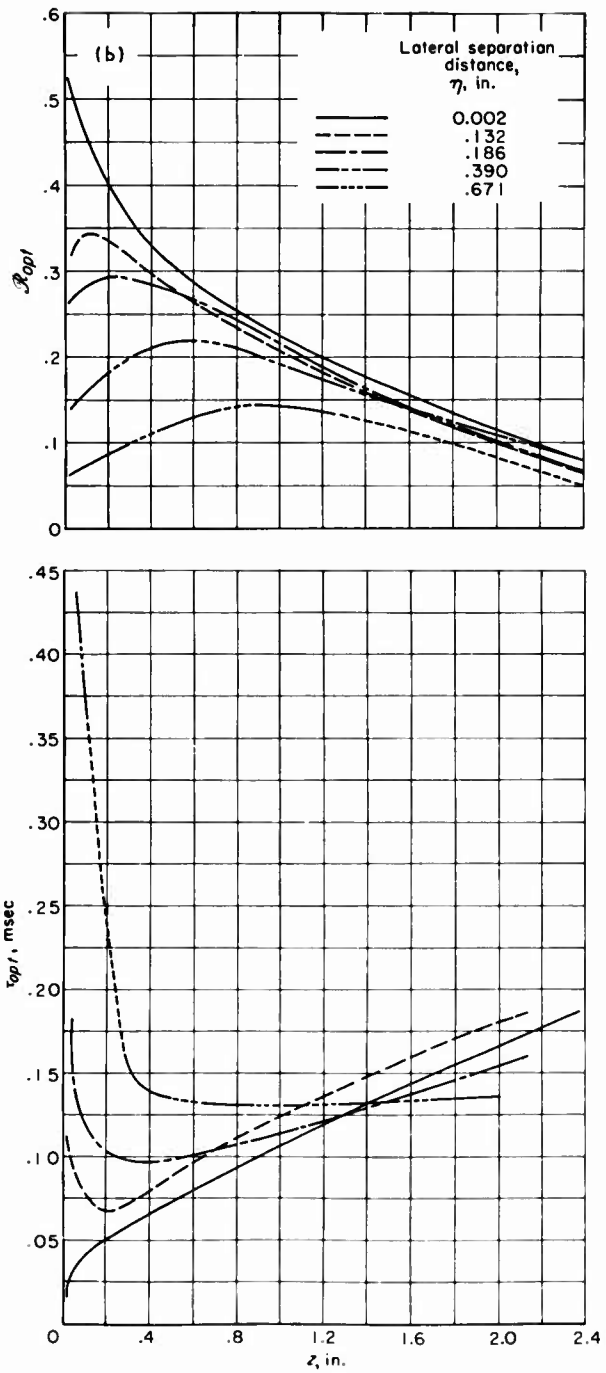

Fig. 27(b) Significant characteristics obtained from correlation of velocity fluctuations with wall-pressure fluctuations, transducer ZS . $\xi \approx 0$

(See also next page)

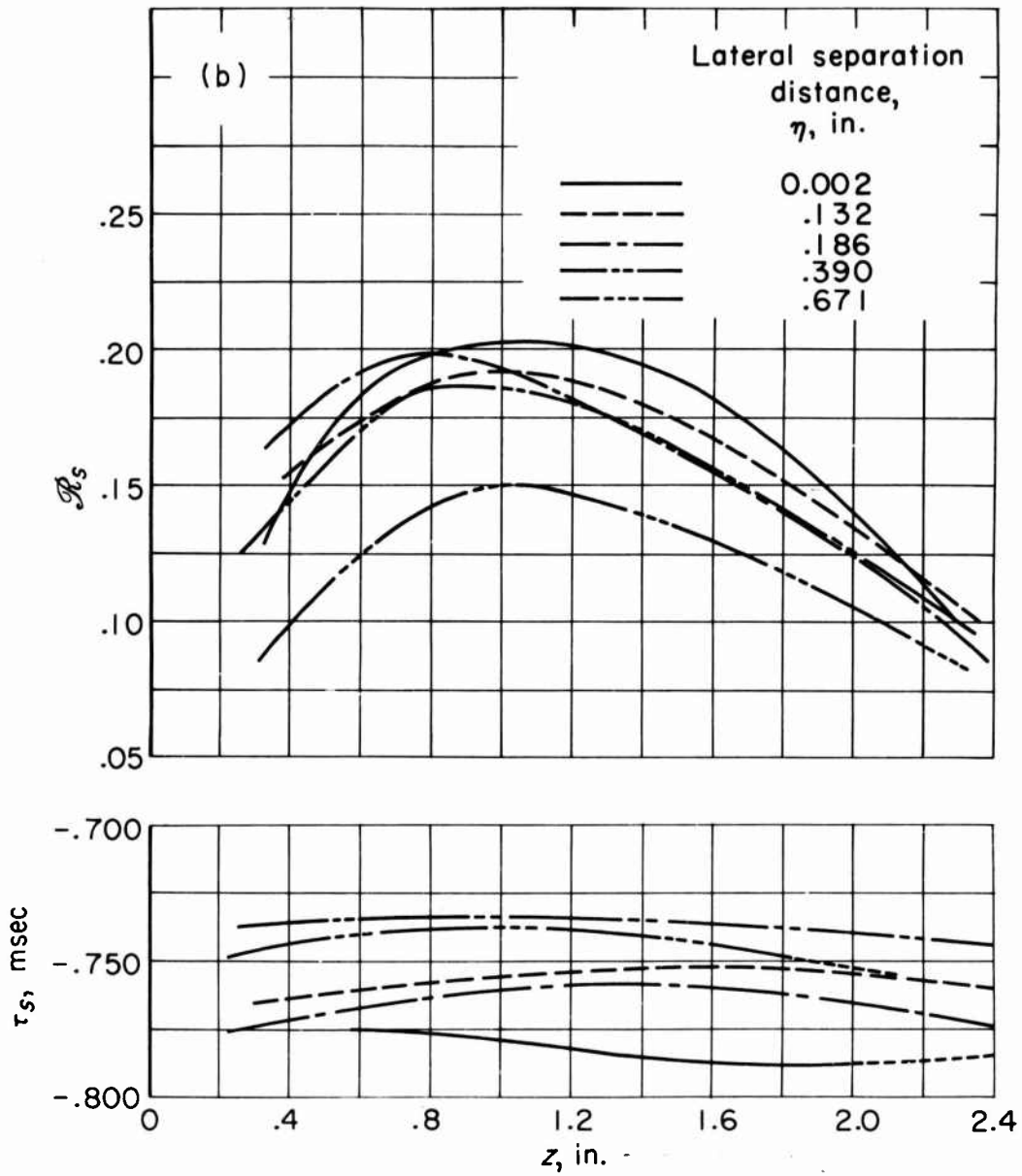

Fig. 27(b) (continued) Significant characteristics obtained from correlations of velocity fluctuations with wall-pressure fluctuations, transducer ZS . $\xi \approx 0$

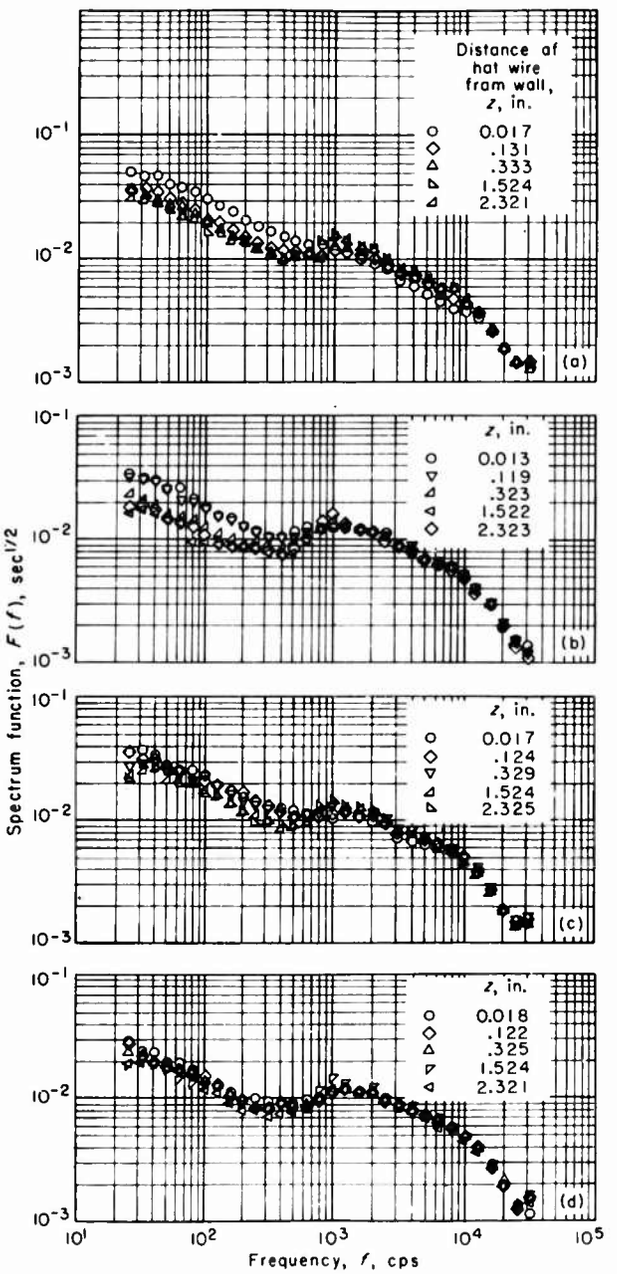

Fig. 28 Spectra of wall-pressure fluctuations, measured by transducer ZS during surveys for correlation data and showing interference effect of hot-wire probe for (a) ξ = -0.001 inch, $\eta \approx 0$; (b) ξ = 0.102 inch, $\eta \approx 0$; (c) ξ = 0.200 inch, $\eta \approx 0$; (d) ξ = 0.307 inch, $\eta \approx 0$

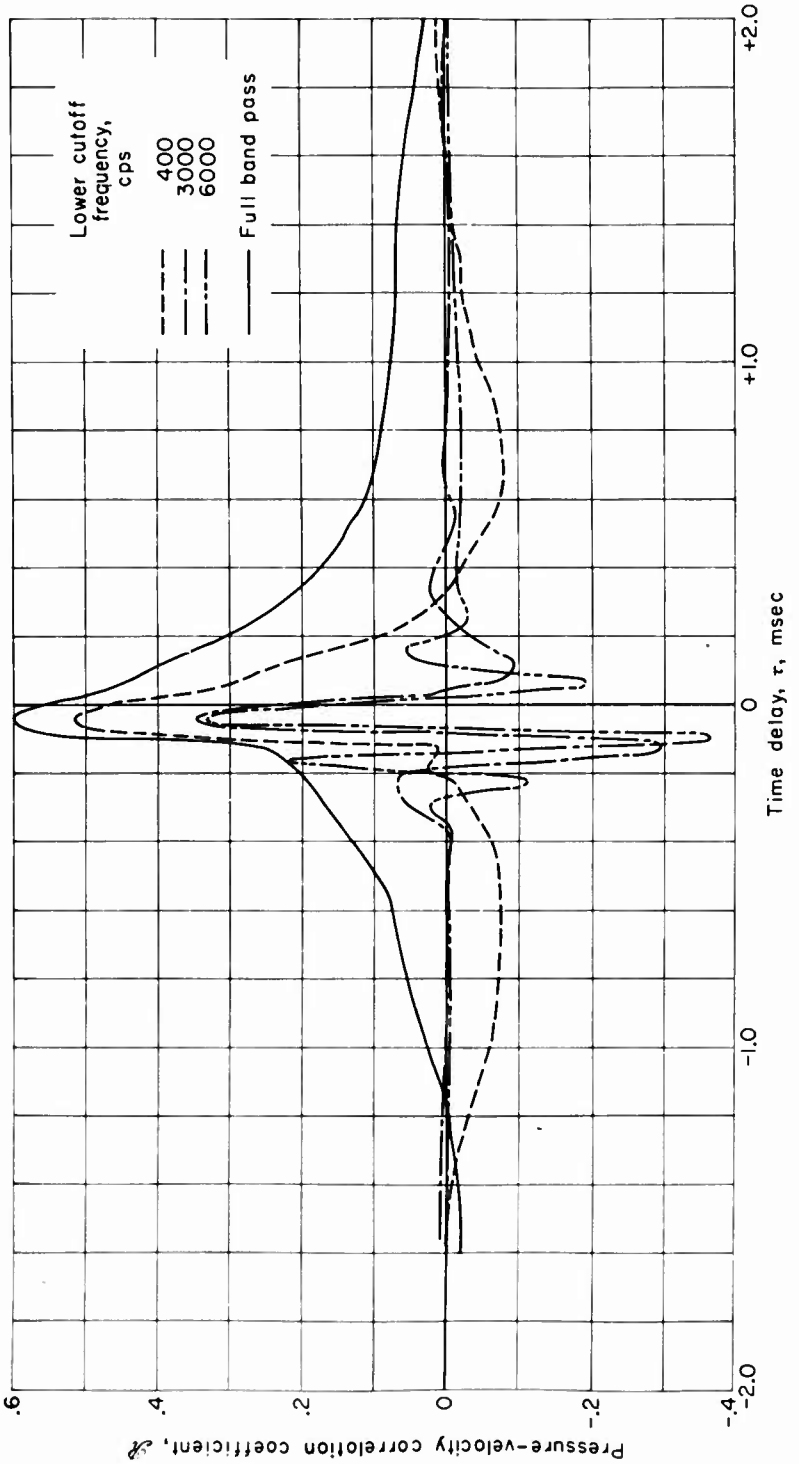

Fig. 29 Effect of high-pass-band filtering on correlation of velocity fluctuations with wall-pressure fluctuations, measured by transducer CB . z = 0.012 inch ; $\xi \approx \eta \approx 0$

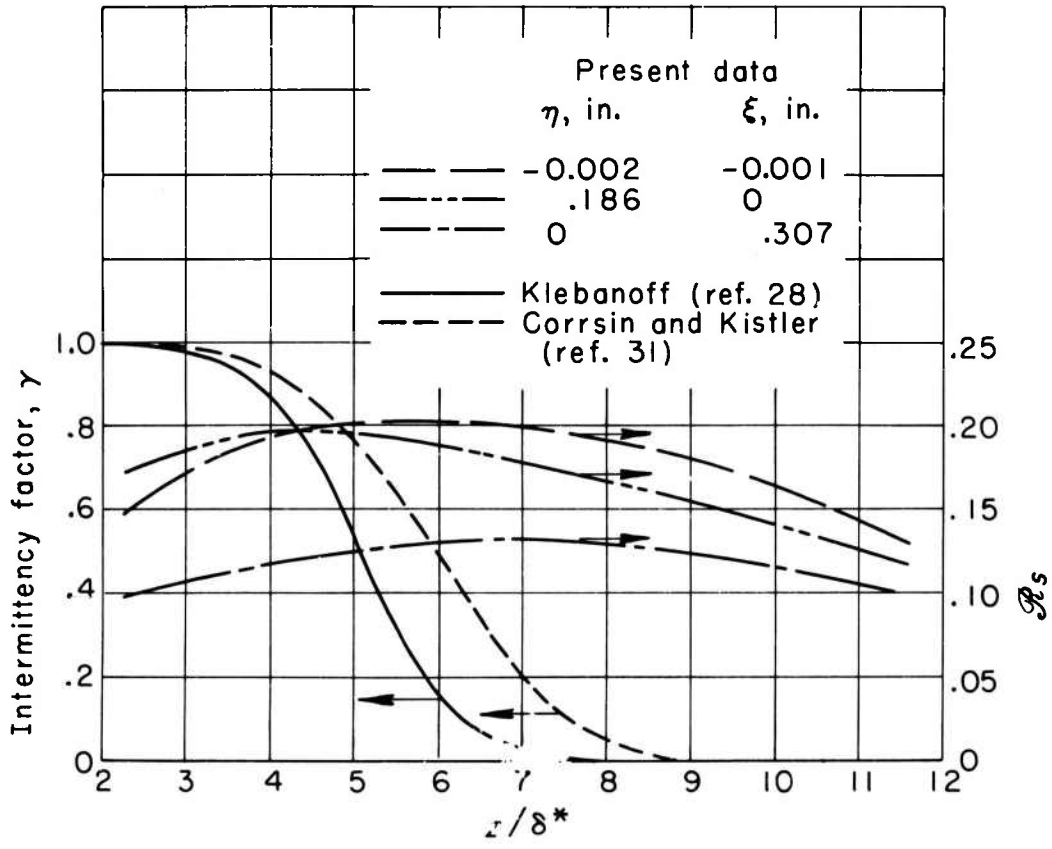

Fig. 30 Comparison of R_s with the intermittency data of Klebanoff[28], and Corrsin and Kistler[31]

DISCUSSION

L.S.G. Kovasznay

Did you attempt to measure space-time correlation with filtered signals? This would remove the anomaly due to the spatial filtering effect of the two transducer configurations.

Author's reply

Due to lack of time in my program, I did not attempt to measure the space-time correlations with narrow-band frequency filtering. However, this 'spatial filtering effect', as you term it, can be interpreted as a wave-number filtering of the data as opposed to the conventional filtering out of bands of the frequency spectrum. Thus, the 'spatial filtering effect' is not an anomaly in the true sense of the word.

DISTRIBUTION

Copies of AGARD publications may be obtained in the various countries at the addresses given below.

On peut se procurer des exemplaires des publications de l'AGARD aux adresses suivantes.

BELGIUM BELGIQUE	Centre National d'Etudes et de Recherches Aéronautiques 11, rue d'Egmont, Bruxelles
CANADA	Director of Scientific Information Service Defense Research Board Department of National Defense 'A' Building, Ottawa, Ontario
DENMARK DANEMARK	Military Research Board Defense Staff Kastellet, Copenhagen Ø
FRANCE	O.N.E.R.A. (Direction) 25, Avenue de la Division Leclerc Châtillon-sous-Bagneux (Seine)
GERMANY ALLEMAGNE	Zentralstelle für Luftfahrt- dokumentation und -information München 27, Maria-Theresia Str. 21 Attn: Dr. H.J. Rautenberg
GREECE GRECE	Greek National Defense General Staff B. MEO Athens
ICELAND ISLANDE	Director of Aviation c/o Flugrad Reykjavik
ITALY ITALIE	Ufficio del Generale Ispettore del Genio Aeronautico Ministero Difesa Aeronautica Roma
LUXEMBURG LUXEMBOURG	Obtainable through Belgium
NETHERLANDS PAYS BAS	Netherlands Delegation to AGARD Michiel de Ruyterweg 10 Delft

NORWAY NORVEGE	Mr. O. Blichner Norwegian Defence Research Establishment Kjeller per Lillestrom
PORTUGAL	Col. J.A. de Almeida Viama (Delegado Nacional do 'AGARD') Direcção do Serviço de Material da F.A. Rua da Escola Politecnica, 42 Lisboa
TURKEY TURQUIE	Ministry of National Defence Ankara Attn. AGARD National Delegate
UNITED KINGDOM ROYAUME UNI	Ministry of Aviation T.I.L., Room 009A First Avenue House High Holborn London W.C.1
UNITED STATES ETATS UNIS	National Aeronautics and Space Administration (NASA) 1520 H Street, N.W. Washington 25, D.C.

Printed by Technical Editing and Reproduction Ltd
Harford House, 7-9 Charlotte St. London. W. 1.

AGARD Report 453 North Atlantic Treaty Organization, Advisory Group for Aeronautical Research and Development WALL-PRESSURE FLUCTUATIONS AND PRESSURE-VELOCITY CORRELATIONS IN TURBULENT BOUNDARY LAYERS John S. Serafini 1963 63 pages, incl. 38 refs., 30 figs & discussion Pressure fluctuations of a turbulent layer along a plane boundary have been investigated experimentally. All measurements were made at a nominal free-stream Mach number of 0.6 and an average Reynolds number per foot of 3.45×10^6 in a wind-tunnel facility specially designed for the purpose. The pressure fluctuations were measured witb P.T.O.	532.526.4 3b2f:3b2ela	AGARD Report 453 North Atlantic Treaty Organization, Advisory Group for Aeronautical Research and Development WALL-PRESSURE FLUCTUATIONS AND PRESSURE-VELOCITY CORRELATIONS IN TURBULENT BOUNDARY LAYERS John S. Serafini 1963 63 pages, incl. 38 refs., 30 figs & discussion Pressure fluctuations of a turbulent layer along a plane boundary bave been investigated experimentally. All measurements were made at a nominal free-stream Mach number of 0.6 and an average Reynolds number per foot of 3.45×10^6 in a wind-tunnel facility specially designed for the purpose. Tbe pressure fluctuations were measured witb P.T.O.	532.526.4 3b2f:3b2ela
AGARD Report 453 North Atlantic Treaty Organization, Advisory Group for Aeronautical Research and Development WALL-PRESSURE FLUCTUATIONS AND PRESSURE-VELOCITY CORRELATIONS IN TURBULENT BOUNDARY LAYERS John S. Serafini 1963 63 pages, incl. 38 refs., 30 figs & discussion Pressure fluctuations of a turbulent layer along a plane boundary have been investigated experimentally. All measurements were made at a nominal free-stream Mach number of 0.6 and an average Reynolds number per foot of 3.45×10^6 in a wind-tunnel facility specially designed for tbe purpose. The pressure fluctuations were measured with P.T.O.	532.526.4 3b2f:3b2ela	AGARD Report 453 North Atlantic Treaty Organization, Advisory Group for Aeronautical Research and Development WALL-PRESSURE FLUCTUATIONS AND PRESSURE-VELOCITY CORRELATIONS IN TURBULENT BOUNDARY LAYERS John S. Serafini 1963 63 pages, incl. 38 refs., 30 figs & discussion Pressure fluctuations of a turbulent layer along a plane boundary have been investigated experimentally. All measurements were made at a nominal free-stream Mach number of 0.6 and an average Reynolds number per foot of 3.45×10^6 in a wind-tunnel facility specially designed for tbe purpose. The pressure fluctuations were measured with P.T.O.	532.526.4 3b2f:3b2ela

miniature pressure transducers and the velocity fluctuations with hot-wire anemometers.

This Report is one in the Series 448-469 inclusive, presenting papers, with discussions, given at the AGARD Specialists' Meeting on 'The Mechanism of Noise Generation in Turbulent Flow' at the Training Center for Experimental Aerodynamics, Rhode-Saint-Genèse, Belgium, 1-5 April 1963, sponsored by the AGARD Fluid Dynamics Panel.

miniature pressure transducers and the velocity fluctuations with hot-wire anemometers.

This Report is one in the Series 448-469 inclusive, presenting papers, with discussions, given at the AGARD Specialists' Meeting on 'The Mechanism of Noise Generation in Turbulent Flow' at the Training Center for Experimental Aerodynamics, Rhode-Saint-Genèse, Belgium, 1-5 April 1963, sponsored by the AGARD Fluid Dynamics Panel.

miniature pressure transducers and the velocity fluctuations with hot-wire anemometers.

This Report is one in the Series 448-469 inclusive, presenting papers, with discussions, given at the AGARD Specialists' Meeting on 'The Mechanism of Noise Generation in Turbulent Flow' at the Training Center for Experimental Aerodynamics, Rhode-Saint-Genèse, Belgium, 1-5 April 1963, sponsored by the AGARD Fluid Dynamics Panel.

miniature pressure transducers and the velocity fluctuations with hot-wire anemometers.

This Report is one in the Series 448-469 inclusive, presenting papers, with discussions, given at the AGARD Specialists' Meeting on 'The Mechanism of Noise Generation in Turbulent Flow' at the Training Center for Experimental Aerodynamics, Rhode-Saint-Genèse, Belgium, 1-5 April 1963, sponsored by the AGARD Fluid Dynamics Panel.

AGARD Report 453 North Atlantic Treaty Organization, Advisory Group for Aeronautical Research and Development WALL-PRESSURE FLUCTUATIONS AND PRESSURE-VELOCITY CORRELATIONS IN TURBULENT BOUNDARY LAYERS John S. Serafini 1963 63 pages, incl. 38 refs., 30 figs & discussion Pressure fluctuations of a turbulent layer along a plane boundary have been investigated experimentally. All measurements were made at a nominal free-stream Macb number of 0.6 and an average Reynolds number per foot of 3.45×10^6 in a wind-tunnel facility specially designed for the purpose. Tbe pressure fluctuations were measured witb P.T.O.	532.526.4 3b2f:3b2ela	AGARD Report 453 North Atlantic Treaty Organization, Advisory Group for Aeronautical Research and Development WALL-PRESSURE FLUCTUATIONS AND PRESSURE-VELOCITY CORRELATIONS IN TURBULENT BOUNDARY LAYERS John S. Serafini 1963 63 pages, incl. 38 refs., 30 figs & discussion Pressure fluctuations of a turbulent layer along a plane boundary bave been investigated experimentally. All measurements were made at a nominal free-stream Mach number of 0.6 and an average Reynolds number per foot of 3.45×10^6 in a wind-tunnel facility specially designed for the purpose. The pressure fluctuations were measured with P.T.O.	532.526.4 3b2f:3b2ela
AGARD Report 453 North Atlantic Treaty Organization, Advisory Group for Aeronautical Research and Development WALL-PRESSURE FLUCTUATIONS AND PRESSURE-VELOCITY CORRELATIONS IN TURBULENT BOUNDARY LAYERS John S. Serafini 1963 63 pages, incl. 38 refs., 30 figs & discussion Pressure fluctuations of a turbulent layer along a plane boundary bave been investigated experimentally. All measurements were made at a nominal free-stream Macb number of 0.6 and an average Reynolds number per foot of 3.45×10^6 in a wind-tunnel facility specially designed for tbe purpose. The pressure fluctuations were measured witb P.T.O.	532.526.4 3b2f:3b2ela	AGARD Report 453 North Atlantic Treaty Organization, Advisory Group for Aeronautical Research and Development WALL-PRESSURE FLUCTUATIONS AND PRESSURE-VELOCITY CORRELATIONS IN TURBULENT BOUNDARY LAYERS John S. Serafini 1963 63 pages, incl. 38 refs., 30 figs & discussion Pressure fluctuations of a turbulent layer along a plane boundary bave been investigated experimentally. All measurements were made at a nominal free-stream Mach number of 0.6 and an average Reynolds number per foot of 3.45×10^6 in a wind-tunnel facility specially designed for tbe purpose. Tbe pressure fluctuations were measured with P.T.O.	532.526.4 3b2f:3b2ela

miniature pressure transducers and the velocity fluctuations with hot-wire anemometers.

This Report is one in the Series 448-469 inclusive, presenting papers, with discussions, given at the AGARD Specialists' Meeting on 'The Mechanism of Noise Generation in Turbulent Flow' at the Training Center for Experimental Aerodynamics, Rhode-Saint-Genèse, Belgium, 1-5 April 1963, sponsored by the AGARD Fluid Dynamics Panel.

miniature pressure transducers and the velocity fluctuations with hot-wire anemometers.

This Report is one in the Series 448-469 inclusive, presenting papers, with discussions, given at the AGARD Specialists' Meeting on 'The Mechanism of Noise Generation in Turbulent Flow' at the Training Center for Experimental Aerodynamics, Rhode-Saint-Genèse, Belgium, 1-5 April 1963, sponsored by the AGARD Fluid Dynamics Panel.

miniature pressure transducers and the velocity fluctuations with hot-wire anemometers.

This Report is one in the Series 448-469 inclusive, presenting papers, with discussions, given at the AGARD Specialists' Meeting on 'The Mechanism of Noise Generation in Turbulent Flow' at the Training Center for Experimental Aerodynamics, Rhode-Saint-Genèse, Belgium, 1-5 April 1963, sponsored by the AGARD Fluid Dynamics Panel.

miniature pressure transducers and the velocity fluctuations with hot-wire anemometers.

This Report is one in the Series 448-469 inclusive, presenting papers, with discussions, given at the AGARD Specialists' Meeting on 'The Mechanism of Noise Generation in Turbulent Flow' at the Training Center for Experimental Aerodynamics, Rhode-Saint-Genèse, Belgium, 1-5 April 1963, sponsored by the AGARD Fluid Dynamics Panel.